JCTC Journal of Chemical Theory and Computation

Article

pubs.acs.org/JCTC

Electrostatic Forces: Formulas for the First Derivatives of a Polarizable, Anisotropic Electrostatic Potential Energy Function Based on Machine Learning

Matthew J. L. Mills[†,§] and Paul L. A. Popelier*[,‡]

[†]Manchester Institute of Biotechnology (MIB), University of Manchester, 131 Princess Street, Manchester M1 7DN, Great Britain

[‡]School of Chemistry, University of Manchester, Oxford Road, Manchester M13 9PL, Great Britain

Supporting Information

ABSTRACT: Explicit formulas are derived analytically for the first derivatives of a (i) polarizable, (ii) high-rank multipolar electrostatic potential energy function for (iii) flexible molecules. The potential energy function uses a machine learning method called Kriging to predict the local-frame multipole moments of atoms defined via the Quantum Chemical Topology (QCT) approach. These atomic multipole moments then interact via an interaction tensor based on spherical harmonics. Atom-centered local coordinate frames are used, constructed from the internal geometry of the molecular system. The forces involve derivatives of both this geometric dependence and of the trained kriging models. In the near future, these analytical forces will enable molecular dynamics and geometry optimization calculations as part of the QCT force field.

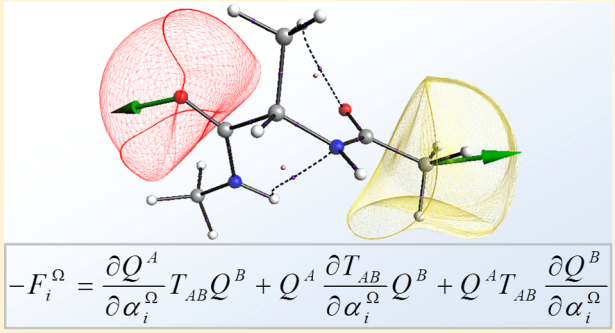

$$-F_i^{\Omega} = \frac{\partial Q^A}{\partial \alpha_i^{\Omega}} T_{AB} Q^B + Q^A \frac{\partial T_{AB}}{\partial \alpha_i^{\Omega}} Q^B + Q^A T_{AB} \frac{\partial Q^B}{\partial \alpha_i^{\Omega}}$$

1. INTRODUCTION

The manner in which the electrostatic interaction is represented in biomolecular simulation has profound consequences for the accuracy of classical force fields (FFs).[1] One area of application where this assertion emerged clearly is that of very long molecular dynamics simulations (100 μs) of proteins.[2] For most of the 24 proteins studied in that work, simulations drifted away from their native structure. The authors stated that "... *it is probably more beneficial in the long run to focus on the development of better force fields than on the development of sophisticated methodologies for scoring structures realized in simulation.*" This is exactly what a relatively small number of research groups around the world are focusing on. The importance of this type of work is vindicated by the fact that very long simulations do not "forget" about the deficiencies of their governing potential by some fortuitous cancellation of errors over very long time scales.

A common and future-proof factor in their approach is the use of multipole moments, which are known[3] to be more realistic than the ubiquitous point charges that are still used in popular force fields. A second common factor of this research effort is the introduction of anisotropic polarizabilities.[4] A *nonexhaustive* list of such next-generation force fields includes NEMO,[5] SIBFA,[6] AMOEBA,[7] XED,[8] EFP,[9] and DMACRYS,[10] while several potentials share the same multipolar philosophy, such as the water potential family ASP-Wn[11] and DPP2,[12] the Gaussian Multipole Model (GMM),[13] and the X-ray crystallography-based Exact Potential Multipole Method (EPMM).[14]

More recently, a novel biomolecular force field,[15,16] currently called QCTFF, is being constructed based on the topological atoms that Quantum Chemical Topology (QCT)[17,18] defines. Topological atoms are finite-volume, malleable boxes that do not overlap, nor do they have gaps between them; they exhaust space and form a mosaic of complementary shapes. Topological atoms change their multipole moments in response to a change in the nuclear configuration of the system they are part of, and so do non-topological atoms (e.g., distributed multipole analysis-based multipole moments[19]). This cause-and-effect relationship was first captured by a machine learning method called Kriging[20,21] for intermolecular geometry changes in water clusters[22] and later for intramolecular conformational changes in a proof-of-concept study on ethanol.[23] A subsequent study on doubly peptide-capped alanine[24] constructed a single Kriging model for 29 local energy minima found in the Ramachandran map based on a training set of 2900 geometries (100 normal-mode distorted geometries for each minimum). The Kriging method handled polarization of atomic multipole moments to quadrupole moment, leading to an average error of 7 kJ mol^{-1} for the overall interatomic electrostatic interaction. This was later improved for histidine[25] (which has more atoms than alanine) to the subkilocalorie-per-mole value of 2.5 kJ mol^{-1}. For larger molecular distortions, unpublished work from our group reports average errors in the range of 2.8 to 5.3 kJ mol^{-1} for all 20 naturally occurring amino acids (capped by a

Received: July 3, 2014
Published: August 14, 2014

dx.doi.org/10.1021/ct500565g | J. Chem. Theory Comput. 2014, 10, 3840−3856

peptide bond at both sides). We also showed[26] that Kriging models were able to predict the electrostatic interaction energy between an ion and all water atoms within 4 kJ mol^{-1} for any one of an external test set of $Na^+(H_2O)_6$ configurations. It should be pointed out, beside other recent use[27−29] of kriging in the area of potential fitting, neural networks[30−32] are an alternative method to capture polarization effects.

The second strand in the QCTFF development is that of molecular dynamics simulations, with high-rank (nonpolarizable) multipolar electrostatics (up to hexadecupole moment) on pure liquids such as water,[33−35] imidazole,[36] and HF,[37] as well as aqueous solutions such as those of imidazole[38] and serine.[39] For all systems, *qualitative* differences were found in the spatial distribution functions calculated from the multipolar electrostatics compared to those calculated from traditional point-charge electrostatics. The multipolar molecular dynamics simulations were carried out within the rigid body formalism[40] and without polarization. In this paper we aim to change both, that is, enable fully flexible (multipolar) simulations with polarization. With this work we demonstrate how to calculate, analytically, the electrostatic forces acting on the nuclei of atoms whose charge distributions are described by multipole moments of arbitrary rank. In a further stage this breakthrough will have to be combined with methods that incorporate the environment[41,42] beyond the simulation box.

2. BACKGROUND: MULTIPOLAR ATOMIC ELECTROSTATIC FORCES

2.1. Multipole Moments and Atomic Local Frames. Unlike point-charges, multipole moments are directional quantities, which therefore need an axis system to be determined. In principle, one could have the global axis system fulfill this role, but we choose instead a local axis system, centered on the atom in question. This local axis system "travels" with the molecule as it translates, but more importantly, also as it rotates with respect to the global axis system. As a result, atomic multipole moments (AMMs) do not change upon rotation of the whole molecule, provided the electron density of that molecule does not change. The task of the Kriging procedure is to capture how AMMs change as a function of atomic positions. Kriging should not be wasted on capturing a change in AMMs simply caused by molecular rotation. Such a rotation can be simply expressed by a rotation matrix and does not need an advanced machine learning method to do the same. Instead, Kriging should focus on the change of AMMs *internally*, within the molecule, as it changes its internal geometry. In other words, it is better to use Kriging to capture the much more complicated link between the electron density and the internal coordinates of a molecule. In summary, the discussion above justifies the choice of a local axis system (versus the global one).

Acting on the decision to formulate Kriging with respect to a local axis system we introduce the atomic local frame (ALF). Each atom of a given molecule has a different ALF, each time centered on the atom in question. Figure 1 illustrates how a typical (right-handed) ALF is constructed, for the example molecule *N*-methylacetamide.

The *x*-axis is chosen to point along the line from the origin atom, denoted Ωo and at position $\mathbf{R}^{\Omega o}$, to the heaviest atom bonded to it, denoted Ωx and at position $\mathbf{R}^{\Omega x}$. The *xy*-plane is defined so as to contain both the heaviest and second heaviest atoms bonded to the origin atom, denoted Ωxy and at position $\mathbf{R}^{\Omega xy}$. In the case of terminal atoms, the *x*-axis is defined by the only atom bonded to the origin atom, and the *xy*-plane is defined to contain the *x*-axis atom and its own heaviest bonding partner. Where two or more duplicate elements are bonded to a central atom, the Cahn−Ingold−Prelog rules are employed to decide priority. When all atoms are equivalent in priority according to these rules then the lowest numbered among them is chosen. Finally, the *z*-axis is constructed such as to lie orthogonal to the *xy*-plane, forming a right-handed ALF.

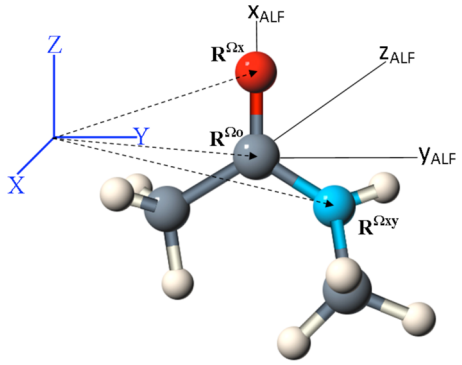

Figure 1. Local axis system (ALF) and global axis system (top left, blue) for the carbonyl carbon in *N*-methylacetamide.

The AMMs can now be defined with respect to each ALF. We prefer to work with AMMs defined by spherical tensors[43,44] rather than by Cartesian tensors because the former are irreducible and hence more compact. For example, for a rank l= 3 AMM (i.e., octupole moment) there are only 7 (= $2l$ + 1) components in the spherical tensor formalism but 27 (=3^l) components in the Cartesian one. The spherical tensor formalism can also be mapped onto the familiar hydrogen-like orbitals of quantum physics, but to avoid confusion it should be kept in mind that our approach is based on the electron density rather than orbitals.

This paper contains many symbols so it is important to define clearly their meaning upfront, starting with the multipole moment notation. Vector components are always written as subscripts, while superscripts always refer to the atom the vector (or scalar) is associated with. For example, an AMM, denoted Q, of rank l = 2 (quadrupole moment) has five components, marked by the index m. If this quadrupole moment is centered on atom A then its m^{th} component is written Q^A_{2m}.

The global frame acts as the reference for any atom in the molecule and can be positioned and oriented arbitrarily. The Cartesian coordinates defined with respect to this global frame are written as α_i, where i = 1, 2, 3 correspond to the familiar x, y, and z, respectively. Each nucleus of a system is the center of an ALF. An ALF effectively describes the electron density of the corresponding atom via the AMMs, denoted Q_{lm}, which are centered at its origin. It is important to realize that the AMMs are defined with respect to a local frame (i.e., an ALF) and not the global frame. As a result, the rotation of an atom (provided it lies within a rigid molecule whose electron density remains fixed, i.e., there is no intermolecular polarization) causes its AMMs to be invariant because the ALF rotates with it. This would not be so if the AMMs were defined with respect to the global frame.

2.2. The Effect of Polarization from the Machine Learning Method Kriging. Traditional polarization methods yield an explicit polarizability (typically denoted α), which expresses the propensity of an electron distribution to deform

dx.doi.org/10.1021/ct500565g | J. Chem. Theory Comput. 2014, 10, 3840−3856

when in an electric field. The proposed method does not return such explicit polarizabilities, but instead predicts the *result* of the polarization process. In other words, we are interested in knowing the values of the AMMs themselves rather than the response function that creates them. Imagine a molecular configuration changing into a previously unseen configuration, and hence electron density. Can one predict the AMMs for each atom in this molecular configuration directly from its nuclear coordinates? The answer is yes, and this is achieved through a machine learning method called Kriging,[21] also known as Gaussian process regression.

Kriging is a stochastical interpolation technique, used here to make predictions for previously unseen molecular geometries spanned by a set of training molecular geometries. Kriging originates in geostatistics[20] and solves the problem of estimating the quantities of some precious material at locations different to those where the concentration of this material had been measured. Kriging succeeds in mapping a given input to a given output, such that it can make predictions of the output values *outside* the original training set. In our application, the input consists of a vector containing $3N_{\text{atom}} - 6$ internal coordinates. In machine learning language, inputs are called *features*. The output is an AMM of interest. We have published the mathematical details of the Kriging method several times before (see for example ref.[25] and the Supporting Information of ref.[22]), which is why we only repeat the key equations here.

We can make a prediction of the output at a new input point $\mathbf{x}^*$ (i.e., molecular geometry) with a trained Kriging model via eq 1,

$$\hat{y}(\mathbf{x}^*) = \hat{\mu} + \sum_{j=1}^{N_{\text{ex}}} a_j \varphi(\mathbf{x}^* - \mathbf{x}^j) \tag{1}$$

where N_{ex} is the number of training examples, $\mathbf{x}^j$ is the vector containing all the features values making up the j^{th} molecular geometry, μ is a constant "background" term modeling the global trend of the observable y, a_i is the j^{th} element of the vector $\mathbf{a} = \mathbf{R}^{-1}(\mathbf{y} - \mathbf{1}\mu)$, while $\varphi(\mathbf{x}^* - \mathbf{x}^i)$ is the j^{th} element of $\mathbf{r}$, which is calculated via eq 2,

$$\mathbf{r} = \{\text{cor}[\varepsilon(\mathbf{x}^*), \varepsilon(\mathbf{x}^1)], \text{cor}[\varepsilon(\mathbf{x}^*), \varepsilon(\mathbf{x}^2)], \ldots, \text{cor}[\varepsilon(\mathbf{x}^*), \varepsilon(\mathbf{x}^n)]\}' \tag{2}$$

where an element of the correlation matrix $\mathbf{R}$ is defined as

$$R_{mn} = \text{cor}[\varepsilon(\mathbf{x}^m), \varepsilon(\mathbf{x}^n)] = \exp[-\sum_{h=1}^{N_{\text{feat}}} \lambda_h |x_h^m - x_h^n|^{p_h}] \tag{3}$$

and where the number of features N_{feat} is the dimensionality of the input space, and m and n index a pair of training examples. The parameters λ_h express the relevance of each input dimension h in explaining the variation in the output variable y. The second set of parameters, denoted p_h, relates to the smoothness of the function in coordinate direction h. The λ_h and p_h parameters are optimized such that the mean squared error of prediction of the Kriging estimator is minimized. The ε quantities may be viewed as normally distributed random variables (with mean zero). They are "error terms" compensating for the inadequacy of the global term in modeling the observed values exactly. The power of Kriging lies in the fact that ε can actually be viewed as essentially coinciding with the prediction of the y output itself. The central assumption in Kriging is that, if two input points are very close together in space, their output values are also similar. Equation 3 formalizes this assumption, because two identical input vectors will cause the exponential's argument to become zero, leading to a maximum correlation of unity. Conversely, the more distant the input vectors the more negative the exponential's argument, and hence the correlation approaches zero.

Note that the parameters λ_h ($\lambda_h \geq 0$) and p_h ($1 \leq p_h \leq 2$) can be written as N_{feat}-dimensional vectors $\boldsymbol{\lambda}$ and $\mathbf{p}$. The dimensionality of the feature space is an important consideration when building models. Higher-dimensional relationships are more difficult to model, so N_{feat} should be minimized where possible. However, Kriging is able to cope well with high values of N_{feat}, so large systems can be treated. A second note concerns the architecture of the optimization protocol. The parameters $\boldsymbol{\lambda}$ and $\mathbf{p}$ of the multivariate Gaussian distribution in eq 3 have been optimized such that so-called likelihood of the observed training data is maximized, a result obtained analytically. Then the likelihood (in fact its logarithm) is maximized but now as a function of $\boldsymbol{\lambda}$ and $\mathbf{p}$. Although this process can also be done analytically via first (and even second) derivatives (research in progress) it is more typically accomplished by genetic algorithms, the branch-and-bound algorithm or simply the Nelder−Mead (or simplex) algorithm. In our work we use partical swarm optimization (PSO), which needs a proper initialization of the search space, currently done by using a Sobol sequence. PSO then moves a population of candidate solutions in ($\boldsymbol{\lambda}$, $\mathbf{p}$)-search-space according to simple formulas over the position and velocity of the various potential solutions. Each solution's movement is influenced by its *local* best position known while it is also guided to the best known positions in the search-space, which are updated as better positions are found by other solutions. Finally, we note that in the test example discussed below no statistical method was applied to prevent overfitting, because the ratio of the number of data points compared to the number of features is safe. Future research will elaborate on the matter of possible overfitting, which we believe does not affect this test case.

2.3. Definition of Features. The choice of the internal coordinates (i.e., features) has repercussions for the details of partial derivatives of the features with respect to the Cartesian displacement coordinates. This is one reason why a separate, albeit brief, section is devoted to these details, although we also consider this necessary because the notation is central to the mathematical derivations following later. We refer again to Figure 1 where the installation of an ALF is made clear.

In a nonlinear molecular there are $3N_{\text{atom}} - 6$ internal degrees of freedom, which are the only ones we focus on. As a result there are $N_{\text{feat}} = 3N_{\text{atom}} - 6$ features. There are two sets of features, each characterized by different mathematical details. The first set consists of three features, and these are associated with the ALF atoms. The second set consists of $3N_{\text{atom}} - 9$ features, and these are associated with the non-ALF atoms. Clearly the total number of features of $3N_{\text{atom}} - 6$ is recovered. The first three atoms are used to fix the ALF itself, and are hence called ALF atoms. The very first feature of the feature vector is the distance between the first atom (the origin) and the second atom, which fixes the x-axis of the ALF. This first feature is denoted $R^{\text{A}x}$. The second feature is the distance between the origin atom and the third atom, which fixes the xy-plane. This feature is denoted $R^{\text{A}xy}$. The third feature is the angle between the two vectors whose distances appeared as the first two features. The third feature is denoted χ^{A}.

dx.doi.org/10.1021/ct500565g | J. Chem. Theory Comput. 2014, 10, 3840−3856

The remaining $N_{atom} - 3$ atoms are non-ALF atoms, and their coordinates are expressed with respect to the (just constructed) ALF. We simply use spherical polar coordinates to describe the non-ALF atoms, which are comprised of a (radial) distance R (from the origin atom), the polar angle θ, and the azimuthal angle φ. For the non-ALF atom An this triplet of features is denoted $\{R^{An}, \theta^{An}, \phi^{An}\}$, and in total there are $3(N_{atom} - 3) = 3N_{atom} - 9$ such features. In summary, the feature vector has the following components: $\{R^{Ax}, R^{Axy}, \chi^{A}, R^{A4}, \theta^{A4}, \phi^{A4}, R^{A5}, \theta^{A5}, \phi^{A5}, ..., R^{AN_{atom}}, \theta^{AN_{atom}}, \phi^{AN_{atom}}\}$.

2.4. Generalities on Energy and Forces. It should be emphasized that we restrict the whole discussion to the electrostatic potential energy only. This quantity, when evaluated between two atoms A and B, is denoted E_{AB} and can be written as

$$E_{AB} = \sum_{l_A=0}^{\infty} \sum_{m_A=-l_A}^{l_A} \sum_{l_B=0}^{\infty} \sum_{m_B=-l_B}^{l_B} Q^{A}_{l_A m_A} T^{l_B m_B}_{l_A m_A} Q^{B}_{l_B m_B} \tag{4}$$

where $Q^{A}_{l_A m_A}$ represents the m^{th} component of a rank l AMM centered on atom A, while T is the interaction tensor that expresses the geometry of the interaction between an AMM on atom A and one on atom B. For example, two interacting monopole moments (essentially atomic charges) show an R^{-1} dependence, where R is the internuclear distance. Interactions involving higher rank AMMs introduce angular dependencies in the tensor T, and powers of R with magnitude greater than 1. In practice, the summations over l_A and l_B do not run unbounded but are capped by the overall interaction rank $L = l_A + l_B + 1$. This rank corresponds to the inverse power of R such that the distance dependence for a given interaction is R^{-L}. It has been shown that $L = 5$ is sufficient for many applications.

The total system electrostatic energy can be found by summing the expression in eq 4 over all pairs of interacting atoms

$$E_{system} = \sum_{AB} E_{AB} \tag{5}$$

In this expression, AB refers to a unique, nonequivalent pair of atoms; that is, the pairs BA, AA, and BB are not included to avoid self-interaction or duplication of terms. The electrostatic force acting on an arbitrary atom Ω of the system, along a global Cartesian axis i, is given by the negative gradient of this system's electrostatic potential energy with respect to the corresponding global frame Cartesian coordinate of that atom. There are three such space coordinates α_i, namely, α_1, α_2, and α_3, and hence the force on each atom is a vector with three components. Using this notation, the component of the force F_i^{Ω} on an atom Ω along α_i can be written

$$F_i^{\Omega} = -\frac{\partial}{\partial \alpha_i^{\Omega}} \left[\sum_{AB} \sum_{l_A=0}^{\infty} \sum_{m_A=-l_A}^{l_A} \sum_{l_B=0}^{\infty} \sum_{m_B=-l_B}^{l_B} Q^{A}_{l_A m_A} T_{l_A m_A l_B m_B} Q^{B}_{l_B m_B} \right] \quad i = 1, 2, 3 \tag{6}$$

For ease of reading, E_{AB} can be rewritten suppressing the explicit summations over l_A, l_B, m_A and m_B,

$$E_{AB} = Q^{A} T_{AB} Q^{B} \tag{7}$$

Application of the product rule to the product of three factors making up each term of eq 6 allows the force components to be written in the "master equation," eq 8,

$$F_i^{\Omega} = -\sum_{AB} \left(\frac{\partial Q^{A}}{\partial \alpha_i^{\Omega}} T_{AB} Q^{B} + Q^{A} \frac{\partial T_{AB}}{\partial \alpha_i^{\Omega}} Q^{B} + Q^{A} T_{AB} \frac{\partial Q^{B}}{\partial \alpha_i^{\Omega}} \right) \tag{8}$$

where the summations over l_A, l_B, m_A, and m_B are again implicit. Of these terms, Q^{A} and Q^{B} are predicted by a Kriging model, while T_{AB} is given either by explicit formulas[45] or recurrence relations.[46] The quantity $\partial T_{AB}/\partial \alpha_i^{\Omega}$ has been previously derived[40] and applied[47] for the rigid case in molecular dynamics simulations of pure liquids and aqueous simulations.[33−39] For a rigid-body treatment without polarization the AMMs remain invariant and hence $\partial Q^{A}/\partial \alpha_i^{\Omega} = \partial Q^{B}/\partial \alpha_i^{\Omega} = 0$. In the general case of flexible molecules, and when polarization is included, this is not true anymore. As a result, the first and third terms in eq 8 do not vanish. How can the derivative $\partial Q/\partial \alpha_i^{\Omega}$ be calculated, when only the relationship between Q and internal molecular coordinates are known (embodied in the Kriging models)? The answer is to use the chain rule of calculus to make the link between derivatives with respect to Cartesian displacement coordinates and those with respect to internal molecular coordinates.

3. RESULTS AND DISCUSSION

The master eq 8, which expresses the force in general, governs the behavior of both rigid and flexible molecules. Knowing the derivative of an AMM with respect to displacement is not necessary for the rigid case but is for the flexible case, which we treat in this paper. In our polarization approach, the AMMs are predicted from the set of internal coordinates (i.e., the feature set $\{f_k\}$). The chain rule (of calculus) provides the link between an AMM Q and a Cartesian displacement α_i by introducing these N_{feat} features f_k (input to the Kriging model) as a link,

$$\frac{\partial Q}{\partial \alpha_i^{\Omega}} = \sum_{k=1}^{N_{feat}} \frac{\partial Q}{\partial f_k} \frac{\partial f_k}{\partial \alpha_i^{\Omega}} \tag{9}$$

The factor on the left of each term, $\partial Q/\partial f_k$, represents the derivative of a predicted AMM with respect to a feature f_k. This is the simplest part and is treated in this section. The right-hand factor, $\partial f_k/\partial \alpha_i^{\Omega}$, is much more involved and is treated in the next section (Section 3.2). This factor is purely geometrical and depends on the choice of representation of internal coordinates. This factor also depends on the definition of the ALFs.

3.1. Derivatives of Atomic Multipole Moments, $\partial Q/\partial f_k$. First we focus on $\partial Q/\partial f_k$, which can be treated analytically because of the analytical nature of a Kriging model. The predicted AMM, denoted Q, is given by eq 10, which follows from combining eqs 1−3.

$$Q = \mu + \sum_{j=1}^{N_{ex}} a_j \exp\left(-\sum_{h=1}^{N_{feat}} \lambda_h |f_h^j - f_h|^{p_h}\right) \tag{10}$$

A previously unseen molecular geometry that contains the atom for which the corresponding AMM Q is to be predicted, is completely characterized by the N_{feat} features. More detail on eq 10 is provided in previous publications[22−26] where the practical construction of Kriging models is also discussed.

The derivative of Q with respect to a given feature f_i can be taken directly,

dx.doi.org/10.1021/ct500565g | J. Chem. Theory Comput. 2014, 10, 3840−3856

$$\frac{\partial Q}{\partial f_i} = \sum_{j=1}^{N_{ex}} (a_j(\mathrm{sign}_j)(-\lambda_i p_i |f_i^j - f_i|^{p_i-1}) \times \exp(-\sum_{h=1}^{N_{feat}} \lambda_h |f_h^j - f_h|^{p_h})) \quad (11)$$

where j runs over all training examples. The function *sign* takes into account the cusp in the derivative of the absolute difference in eq 11, and is defined as

$$\mathrm{sign}_j = \begin{cases} 1 & \text{if } f_i^j - f_i \le 0 \\ -1 & \text{if } f_i^j - f_i > 0 \end{cases} \quad (12)$$

A minor technical complication arises because Kriging models are trained using normalized features $\overline{f}_i$, and that they therefore produce normalized output $\overline{Q}$. This means that eq 11 actually calculates $\partial\overline{Q}/\partial\overline{f}_i$ rather than the desired $\partial Q/\partial\overline{f}_i$, although we do not repeat this equation to make this clear. Fortunately, the relation between the latter two quantities is straightforward,

$$\frac{\partial Q}{\partial f_i} = \frac{\partial \overline{Q}}{\partial \overline{f}_i}\left(\frac{Q_{max} - Q_{min}}{f_{max} - f_{min}}\right) \quad (13)$$

and has been derived in Appendix A of the Supporting Information. Adding the two superscript dashes at the left-hand side of eq 11 and then substituting it into eq 13 is sufficient to compute the derivatives of any Kriging model with respect to an arbitrary feature. The first factor of each term in eq 9, $\partial Q/\partial f_k$, can therefore be determined analytically for any system described by any set of features. This factor is separated cleanly from the derivatives of the (geometrical) features themselves with respect to the global Cartesian coordinates of the system, $\partial f_k/\partial\alpha_i^\Omega$. This fact is useful when considering the computation of the atomic forces for features not relating to the ALF, as the formulas in this section hold for any choice of features. The derivatives of the geometrical features for the multipolar FF will be discussed in the next section, for the case of the ALF representation of a system in QCTFF.

3.2. Derivatives of the Features with Respect to the Cartesian Displacement Coordinates, $\partial f_k/\partial\alpha_i^\Omega$. In this section we treat the right-hand factor, $\partial f_k/\partial\alpha_i^\Omega$, of the key equation, eq 9. The systematic calculation of this factor is much more involved but much detail has been decanted in the Supporting Information. It is helpful to refer again to Figure 1 where Ωo, Ωx, and Ωxy marked the three atoms determining the ALF. For our purposes we have to specify Ω to be either A or B. Thus, the ALFs of a pair of interacting atoms A and B can be written as

$$\mathrm{ALF_A} = \{Ao,\ Ax,\ Axy\} \quad \mathrm{ALF_B} = \{Bo,\ Bx,\ Bxy\} \quad (14)$$

The factor $\partial f_k/\partial\alpha_i^\Omega$ involves the derivatives of the features describing the molecule from the perspective of an atom A or B with respect to a global system coordinate of an atom Ω, labeled α_i^Ω. These derivatives have different characteristics depending on whether Ω is used in the definition of the ALFs of atom A, or atom B, or both atoms A and B, or neither. To further illustrate this, it is helpful to write the two AMM derivatives,

$$\frac{\partial Q^A}{\partial \alpha_i^\Omega} = \sum_{k=1}^{N_{feat}} \frac{\partial Q^A}{\partial f_k^A}\frac{\partial f_k^A}{\partial \alpha_i^\Omega} \quad \frac{\partial Q^B}{\partial \alpha_i^\Omega} = \sum_{k=1}^{N_{feat}} \frac{\partial Q^B}{\partial f_k^B}\frac{\partial f_k^B}{\partial \alpha_i^\Omega} \quad (15)$$

The form of the feature derivatives $\partial f_k/\partial\alpha_i^\Omega$ will depend on whether $\Omega \in \mathrm{ALF_A}$ (or equivalently $\Omega \in \mathrm{ALF_B}$). It is sufficient to consider the case for atom A here; the same discussion can be applied to atom B by exchanging the index A for B in all following equations. Note that there is an extra complication: an atom Ω may be simultaneously a member of the ALFs of A and B. This qualification does not need to be considered for the AMM derivatives, $\partial Q^A/\partial\alpha_i^\Omega$, but will be important in evaluating the tensor derivatives $\partial T_{AB}/\partial\alpha_i^\Omega$ in Section 3.4.

We remind ourselves that the full set of features is given by $\{R^{Ax}, R^{Axy}, \chi^A, R^{A4}, \theta^{A4}, \phi^{A4}, R^{A5}, \theta^{A5}, \phi^{A5}, ..., R^{AN_{atom}}, \theta^{AN_{atom}}, \phi^{AN_{atom}}\}$. They describe the molecule from the perspective of atom A and are defined via the following equations,

$$\begin{aligned} R^{Ax} &= \sqrt{(\mathbf{R}^{Ax} - \mathbf{R}^{Ao})^2} \\ R^{Axy} &= \sqrt{(\mathbf{R}^{Axy} - \mathbf{R}^{Ao})^2} \\ \chi^A &= \arccos\frac{\mathbf{R}^{Ax}\cdot\mathbf{R}^{Axy}}{R^{Ax}R^{Axy}} \end{aligned} \quad (16)$$

$$\begin{aligned} R^{An} &= \sqrt{(\mathbf{R}^{An} - \mathbf{R}^{Ao})^2} \\ \theta^{An} &= \arccos\frac{\zeta_3^{An}}{R^{An}} \\ \phi^{An} &= \arctan\frac{\zeta_2^{An}}{\zeta_1^{An}} \\ n &= (4, ..., N_{at}) \end{aligned} \quad (17)$$

where ζ_i^{An} $(i = 1, 2, 3)$ is a Cartesian coordinate expressed in the ALF, and $\mathbf{R}^{Ao}$, $\mathbf{R}^{Ax}$, $\mathbf{R}^{Axy}$, and $\mathbf{R}^{An}$ are position vectors (see Figure 1 for the first three vectors).

We now obtain the derivatives of each of these features (in eqs 16 and 17) with respect to a global Cartesian coordinate α_i^Ω. The detailed derivation is presented in Appendix B of the Supporting Information. The features R^{Ax}, R^{Axy}, and R^{An}, where $n = 2, 3, 4, ..., N_{atom}$, can be treated together. We introduce the more general symbol R^n to mark this type of feature, where the identity of the atom in question has been omitted. This generalized feature R^n represents the distance between an atom n $(n = 2, 3, ..., N_{atom})$ and the origin of the ALF in question. The first result is given in eq 18,

$$\frac{\partial R^n}{\partial \alpha_i^\Omega} = \frac{(\alpha_i^n - \alpha_i^{Ao})}{R^n}\Delta_{\Omega n} \quad (18)$$

where $\Delta_{\Omega n}$ denotes a variant of the usual Kronecker delta symbol δ_{ij}, but now keeps track of a sign, that is,

$$\Delta_{\Omega n} = \begin{cases} -1 & \text{if } \Omega = Ao \\ 1 & \text{if } \Omega = n \end{cases} \quad (19)$$

This covers the derivatives of the first two features and a third of the non-ALF features (i.e., all distances). The next result refers to the third feature, the unique ALF angle and is given in eq 20,

$$\frac{\partial \chi^{A}}{\partial \alpha_i^{\Omega}} = \frac{1}{\sin \chi^{A}}\left[\left(\frac{\mathbf{R}^{Ax}\cdot\mathbf{R}^{Axy}}{R^{Axy}(R^{Ax})^3}\right)(\alpha_i^{Ax} - \alpha_i^{Ao})\Delta_{\Omega Ax} + \left(\frac{\mathbf{R}^{Ax}\cdot\mathbf{R}^{Axy}}{R^{Ax}(R^{Axy})^3}\right)(\alpha_i^{Axy} - \alpha_i^{Ao})\Delta_{\Omega Axy} - \left(\frac{1}{R^{Ax}R^{Axy}}\right)\{(\alpha_i^{Ax} - \alpha_i^{Ao})\Delta_{\Omega Axy} + \Delta_{\Omega Ax}(\alpha_i^{Axy} - \alpha_i^{Ao})\}\right] \tag{20}$$

The next result covers the derivatives of the angular features θ^{An} of the non-ALF atoms, and is given in eq 21,

$$\frac{\partial \theta^{An}}{\partial \alpha_i^{\Omega}} = \frac{1}{\sin \theta^{An}}\left[\frac{\zeta_3^{An}(\alpha_i^{n} - \alpha_i^{Ao})}{(R^{An})^3}\Delta_{\Omega n} - \frac{1}{R^{An}}\frac{\partial \zeta_3^{An}}{\alpha_i^{\Omega}}\right] \tag{21}$$

Note that the second factor of the second term will be described in Section 3.3.

The next and final result covers the derivatives of the angular features ϕ^{An} of the non-ALF atoms, and is given in eq 22,

$$\frac{\partial \phi^{An}}{\partial \alpha_i^{\Omega}} = \cos^2 \phi^{An}\left[\frac{-\zeta_2^{An}}{(\zeta_1^{An})^2}\frac{\partial \zeta_1^{An}}{\partial \alpha_i^{\Omega}} + (1/\zeta_1^{An})\frac{\partial \zeta_2^{An}}{\partial \alpha_i^{\Omega}}\right] \tag{22}$$

Note that again some partial derivatives have not been resolved, that is, the second factor of both terms. They will be described in Section 3.3 (and Appendix C, Supporting Information).

This completes the set of closed form equations needed to calculate the feature derivatives, except for the description of the local frame Cartesian coordinate derivatives, which are given in the following section (and in greater detail in Appendix C, Supporting Information). These results are only applicable to cases where the AMMs of an atom are predicted from vectors of features computed within the ALF description of a molecule as shown in Figure 1.

3.3. Derivatives of Local Frame Cartesian Coordinates, $\partial\zeta_j^{An}/\partial\alpha_i^{\Omega}$. The previous section mentioned unresolved derivatives of the type $\partial\zeta_j^{An}/\partial\alpha_i^{\Omega}$ (j = 1, 2, 3 and i = 1, 2, 3) (see eqs 21 and 22). Here we calculate these derivatives of the Cartesian coordinates expressed in the ALF with respect to the Cartesian displacement coordinates expressed in the global frame. The key to the calculation of these derivatives is the rotation matrix **C** that connects the global frame Cartesian coordinates α_i with the ALF Cartesian coordinates ζ_j. The construction of this 3 × 3 matrix mirrors the construction of an ALF, as briefly explained in connection with Figure 1. Each ALF has its own **C**−matrix.

Emphasizing the different nature of C_{j1}, C_{j2}, and C_{j3} the relation between ζ_j and α_i is then simply

$$\zeta_j^{An} = C_{j1}(\alpha_1^{An} - \alpha_1^{Ao}) + C_{j2}(\alpha_2^{An} - \alpha_2^{Ao}) + C_{j3}(\alpha_3^{An} - \alpha_3^{Ao}) \tag{23}$$

The desired derivative is found by application of the product rule to each term of eq 23 and using eq B4 (from the Supporting Information),

$$\frac{\partial \zeta_j^{An}}{\partial \alpha_i^{\Omega}} = \sum_{k=1}^{3}\frac{\partial C_{jk}}{\partial \alpha_i^{\Omega}}(\alpha_k^{An} - \alpha_k^{Ao}) + \sum_{k=1}^{3} C_{jk}\delta_{ik}\Delta_{\Omega n} \tag{24}$$

Appendix C (Supporting Information) provides the details of the calculation of the three types of derivatives $\partial C_{jk}/\partial\alpha_i^{\Omega}$ (k = 1, 2, 3), while some key (intermediate) results are given here.

We start with the first row of **C** (j = 1), for which we need the explicit form of C_{1k}. The x-axis in the ALF is constructed from the difference in the position vector of *Ax* (atom 2) and *Ao* (atom 1). We remember that rotation matrix **C** consists of unit vectors, so this difference needs to be normalized, or

$$C_{1k} = \frac{(\alpha_k^{Ax} - \alpha_k^{Ao})}{R^{Ax}} \tag{25}$$

Using expressions derived before, we obtain eq 26, which expresses the desired derivative (left-hand side) as a function of nonderivatives,

$$\frac{\partial C_{1k}}{\partial \alpha_i^{\Omega}} = \frac{1}{R^{Ax}}\delta_{ik}\Delta_{\Omega Ax} - \frac{(\alpha_i^{Ax} - \alpha_i^{Ao})(\alpha_k^{Ax} - \alpha_k^{Ao})}{(R^{Ax})^3}\Delta_{\Omega Ax} \tag{26}$$

The second row of **C** (j = 2) is significantly more complicated. The elements of this unit vector can be written

$$C_{2k} = \frac{y_k}{\sqrt{\mathbf{y}\cdot\mathbf{y}}} \tag{27}$$

where **y** is the vector representing the y-axis in the ALF. As explained in connection with Figure 1 it is constructed by forcing it to lie in the xy-plane, which is spanned by atom 2 ($\mathbf{R}^{Ax}$) and atom 3 ($\mathbf{R}^{Axy}$),

$$\mathbf{y} = \sigma\mathbf{R}^{Ax} + \mathbf{R}^{Axy} \tag{28}$$

A calculation given in Appendix C (Supporting Information) gives the derivative of σ as a function of nonderivatives,

$$\frac{\partial \sigma}{\partial \alpha_i^{\Omega}} = -\frac{\mathbf{R}^{Ax}\cdot\mathbf{R}^{Axy}}{(\mathbf{R}^{Ax}\cdot\mathbf{R}^{Ax})^2}2(\alpha_i^{Ax} - \alpha_i^{Ao})\Delta_{\Omega Ax} - \frac{(\alpha_i^{Ax} - \alpha_i^{Ao})\Delta_{\Omega Ax} + (\alpha_i^{Axy} - \alpha_i^{Ao})\Delta_{\Omega Axy}}{\mathbf{R}^{Ax}\cdot\mathbf{R}^{Ax}} \tag{29}$$

The final expression $\partial C_{2k}/\partial\alpha_i^{\Omega}$ is too cumbersome to show here and its derivation is of no practical value. Indeed, for the implementation of this derivative we have written source code that consists of a sequence of nested equations (given in Appendix C, Supporting Information), each of which provides the value to be inserted in the next equation. Such a cascade of evaluations ensures that the final value can be calculated analytically and efficiently.

The same logic applies to the final derivative $\partial C_{3k}/\partial\alpha_i^{\Omega}$. Again, the details are in Appendix C (Supporting Information), but it is worth highlighting that the third row of **C** (j = 3) is associated with the z-axis of the ALF and given by the cross product of rows 1 and 2 of the rotation matrix **C**

$$\mathbf{C}_3 = \mathbf{C}_1 \times \mathbf{C}_2 = (C_{12}C_{23} - C_{13}C_{22})\mathbf{u}_x + (C_{13}C_{21} - C_{11}C_{23})\mathbf{u}_y + (C_{11}C_{22} - C_{12}C_{21})\mathbf{u}_z \tag{30}$$

where $\mathbf{u}_x$, $\mathbf{u}_y$, and $\mathbf{u}_z$ are three mutually orthogonal unit vectors spanning the global frame. A straightforward application of the product rule gives the derivatives of the third row C_{3k} in terms of the previously described derivatives of the first (C_{1k}) and second (C_{2k}) rows.

With this set of equations, the required derivatives of the local frame Cartesian coordinates with respect to the global frame Cartesian coordinates are defined analytically. The

dx.doi.org/10.1021/ct500565g | J. Chem. Theory Comput. 2014, 10, 3840−3856

combination of these expressions with those of the two previous sections (3.1 and 3.2) constitutes a complete description of the computation of the derivatives of the AMMs of a system with respect to the global Cartesian coordinates of the system nuclei, within the ALF formalism.

Returning to the master eq 8, we can now conclude that, via eq 15, the first and third term can be evaluated analytically; the terms dependent on derivatives of AMMs are now completely known. It remains to discuss the central term in eq 8, which requires a description of the computation of the derivatives of the interaction tensor T with respect to the global frame Cartesian nuclear coordinates α, or $\partial T_{AB}/\partial \alpha_i^{\Omega}$.

3.4. Derivatives of Interaction Tensor Components, $\partial T_{AB}/\partial \alpha_i^{\Omega}$. The central term of eq 8 requires the derivatives of the interaction tensor T_{AB} with respect to displacement of a nucleus along a global frame Cartesian coordinate. The tensor will have nonzero derivatives when the atom Ω is involved in defining the ALF of either of the pair of interacting atoms (i.e., A and B). This is so because the tensor components are functions of the internuclear separation and relative orientations of those ALFs.

T_{AB} is conveniently expressed in terms of 16 scalar products, between the interatomic vector, denoted $\mathbf{R}$, and the two sets of unit vectors representing the local axis systems centered on the interacting atoms, $\mathbf{w}_j^A$ and $\mathbf{w}_j^B$ (j = 1, 2, 3), which are expressed in the global reference frame. These 16 quantities are denoted q and consist of: the single quantity $\mathbf{R}\cdot\mathbf{R}$, three quantities of the type $\mathbf{w}_j^A\cdot\mathbf{R}$, three of the type $\mathbf{w}_j^B\cdot\mathbf{R}$, and nine of the type $\mathbf{w}_j^A\cdot\mathbf{w}_k^B$. By expressing the interaction tensor in terms of these 16, it is possible to write the derivative of T_{AB} with respect to a global Cartesian coordinate, α_i^{Ω} (where Ω is any system atom) using the chain rule. The result is

$$\frac{\partial T_{AB}}{\partial \alpha_i^{\Omega}} = \sum_{k=1}^{16} \frac{\partial T_{AB}}{\partial q_k}\frac{\partial q_k}{\partial \alpha_i^{\Omega}} \tag{31}$$

The first factor in each term, $\partial T_{AB}/\partial q_k$, has been previously described for the rigid body case[40] and is detailed later in this section. The description of the second factor, $\partial q_k/\partial \alpha_i^{\Omega}$, is given here for flexible molecules, as it differs from the case of interacting rigid molecules. Three types of derivative arise, as a result of the three types of dot products described above.

3.4.1. Derivatives of Dot Products, $\partial q_k/\partial \alpha_i^{\Omega}$ (k = 1, ..., 16). First, the derivative of the dot product $\mathbf{R}\cdot\mathbf{R}$ of the interatomic vector with itself is the same as in the rigid case because it is a function only of the positions of the two interacting atoms A and B. The dot product can be written in terms of the global frame Cartesian coordinates as

$$\mathbf{R}\cdot\mathbf{R} = \sum_{j=1}^{3} (\alpha_j^B - \alpha_j^A)^2 \tag{32}$$

and the derivative can be taken directly. The result depends on the atom whose coordinate the derivative is to be taken with respect to

$$\begin{aligned}\frac{\partial \mathbf{R}\cdot\mathbf{R}}{\partial \alpha_i^{\Omega}} &= \sum_{j=1}^{3} 2(\alpha_j^B - \alpha_j^A)\frac{\partial(\alpha_j^B - \alpha_j^A)}{\partial \alpha_i^{\Omega}} \\ &= \sum_{j=1}^{3} 2(\alpha_j^B - \alpha_j^A)\Delta_{\Omega}\delta_{ij} \\ &= 2(\alpha_i^B - \alpha_i^A)\Delta_{\Omega}\end{aligned} \tag{33a}$$

$$\Delta_{\Omega} = \begin{cases} -1 & \text{if} \quad \Omega = A \\ 1 & \text{if} \quad \Omega = B \end{cases} \tag{33b}$$

where δ_{ij} is the Kronecker delta discussed in Appendix B (see eq B5, Supporting Information). Derivatives of $\mathbf{R}\cdot\mathbf{R}$ with respect to the Cartesian coordinates of atoms other than the interacting pair (i.e., A and B) are zero, as displacement of such atoms has no effect on the internuclear distance.

The second type of derivative is of the scalar products of $\mathbf{R}$ with the unit vectors of the ALFs, that is, $\mathbf{w}_j^A\cdot\mathbf{R}$ or $\mathbf{w}_j^B\cdot\mathbf{R}$. All of these vectors must first be expressed in a common reference frame (the global frame). The derivation for $\mathbf{w}_j^A\cdot\mathbf{R}$ is given below while the results for $\mathbf{w}_j^B\cdot\mathbf{R}$ can be obtained by substituting A for B in the resulting equations, which are paired up (eqs 38 and 39). Expressed in the global frame, $\mathbf{R}$ is a vector with three components i, each given by

$$R_i = \alpha_i^B - \alpha_i^A \tag{34}$$

Writing the ALF unit vectors with respect to the global frame, $\mathbf{w}_j^A$, requires the rotation matrix from an ALF to the global frame, as well as the unit vectors expressed with respect to the ALF, $\mathbf{u}_j^A$. The rotation matrix that transforms a vector from the global frame to the ALF, $\mathbf{C}$, is described in Section 3.3 and in more detail in Appendix C (Supporting Information). The inverse transformation is described by the inverse of the rotation matrix. The matrix $\mathbf{C}$ is orthogonal, and as such its inverse is given by its transpose, which we denote $\mathbf{D}$. This allows us to write the ALF unit vectors in the global frame as

$$\mathbf{w}_j^A = \mathbf{D}^A\mathbf{u}_j^A \tag{35}$$

The $\mathbf{u}_j^A$ vectors are normalized unit vectors for the ALF axes, and so form a unit matrix allowing the previous equation to be rewritten as

$$\mathbf{w}^A = \mathbf{D}^A\mathbf{1} \tag{36}$$

Thus, the global frame ALF unit vectors are given by the columns of the rotation matrix that transforms a vector expressed in the ALF of an atom A or B to the same vector expressed in the global frame.

$$\mathbf{w}_j^A = (D_{1j}^A, D_{2j}^A, D_{3j}^A)\mathbf{w}_j^B = (D_{1j}^B, D_{2j}^B, D_{3j}^B) \tag{37}$$

The scalar products $\mathbf{w}_j^A\cdot\mathbf{R}$ and $\mathbf{w}_j^B\cdot\mathbf{R}$ can be expressed in terms of the global frame nuclear coordinates and rotation matrix elements

$$\begin{aligned}\mathbf{w}_j^A\cdot\mathbf{R} = {} & D_{1j}^A(\alpha_1^B - \alpha_1^A) + D_{2j}^A(\alpha_2^B - \alpha_2^A) \\ & + D_{3j}^A(\alpha_3^B - \alpha_3^A)\end{aligned} \tag{38a}$$

$$\begin{aligned}\mathbf{w}_j^B\cdot\mathbf{R} = {} & D_{1j}^B(\alpha_1^B - \alpha_1^A) + D_{2j}^B(\alpha_2^B - \alpha_2^A) \\ & + D_{3j}^B(\alpha_3^B - \alpha_3^A)\end{aligned} \tag{38b}$$

This allows the required derivatives to be taken via the product rule, resulting in two types of term,

$$\begin{aligned}\frac{\partial \mathbf{w}_j^A\cdot\mathbf{R}}{\partial \alpha_i^{\Omega}} = {} & D_{ij}^A\frac{\partial(\alpha_i^B - \alpha_i^A)}{\partial \alpha_i^{\Omega}} + \left(\frac{\partial D_{1j}^A}{\partial \alpha_i^{\Omega}}(\alpha_1^B - \alpha_1^A)\right. \\ & \left. + \frac{\partial D_{2j}^A}{\partial \alpha_i^{\Omega}}(\alpha_2^B - \alpha_2^A) + \frac{\partial D_{3j}^A}{\partial \alpha_i^{\Omega}}(\alpha_3^B - \alpha_3^A)\right)\end{aligned} \tag{39a}$$

dx.doi.org/10.1021/ct500565g | J. Chem. Theory Comput. 2014, 10, 3840−3856

$$\frac{\partial \mathbf{w}_j^{\mathrm{B}}\cdot\mathbf{R}}{\partial \alpha_i^{\Omega}} = D_{ij}^{\mathrm{B}}\frac{\partial(\alpha_i^{\mathrm{B}} - \alpha_i^{\mathrm{A}})}{\partial \alpha_i^{\Omega}} + \left(\frac{\partial D_{1j}^{\mathrm{B}}}{\partial \alpha_i^{\Omega}}(\alpha_1^{\mathrm{B}} - \alpha_1^{\mathrm{A}}) + \frac{\partial D_{2j}^{\mathrm{B}}}{\partial \alpha_i^{\Omega}}(\alpha_2^{\mathrm{B}} - \alpha_2^{\mathrm{A}}) + \frac{\partial D_{3j}^{\mathrm{B}}}{\partial \alpha_i^{\Omega}}(\alpha_3^{\mathrm{B}} - \alpha_3^{\mathrm{A}})\right) \tag{39b}$$

Note that the first term in eqs 39a and 39b was obtained by using

$$\frac{\partial(\alpha_j^{\mathrm{B}} - \alpha_j^{\mathrm{A}})}{\partial \alpha_i^{\Omega}} = 0 \text{ if } i \neq j \;\forall\; \Omega \tag{40}$$

such that the only D_{kj}^{A} (k = 1, 2, 3) that survives is the one where $k = i$. This first type of term is in fact simply the derivative of a component of **R** with respect to a global Cartesian coordinate. As **R** is expressed in the global frame, the corresponding derivative is readily obtained from eq 34,

$$\frac{\partial R_i}{\partial \alpha_i^{\Omega}} = \frac{\partial(\alpha_i^{\mathrm{B}} - \alpha_i^{\mathrm{A}})}{\partial \alpha_i^{\Omega}} = \begin{cases} -1 & \text{if} \quad \Omega = A \\ 1 & \text{if} \quad \Omega = B \\ 0 & \text{if} \quad \Omega \neq A, B \end{cases} \tag{41}$$

For all atoms Ω other than A and B this derivative is zero.

The second type of term in eqs 39a, 39b involves the derivative of the rotation matrix elements D_{kj} with respect to a global Cartesian coordinate α_i, as described in Section 3.3 on local frame coordinate derivatives. In the case of interacting rigid bodies these terms equal zero.

Third and finally, the derivative of the scalar product of two ALF unit vectors, $\mathbf{w}_j^{\mathrm{A}}\cdot\mathbf{w}_k^{\mathrm{B}}$, is to be described. The scalar product can be written, again expressing all vectors in the global frame, as a sum of products of rotation matrix elements. Using the product rule the derivatives can be written in terms of the elements of each atom's rotation matrices, **D**, and their derivatives with respect to the global Cartesian coordinates. The computation of both such quantities is described in Section 3.3 on local coordinate derivatives. The dot product is written

$$\mathbf{w}_j^{\mathrm{A}}\cdot\mathbf{w}_k^{\mathrm{B}} = D_{1j}^{\mathrm{A}}D_{1k}^{\mathrm{B}} + D_{2j}^{\mathrm{A}}D_{2k}^{\mathrm{B}} + D_{3j}^{\mathrm{A}}D_{3k}^{\mathrm{B}} \tag{42}$$

and the required derivatives are then given by application of the product rule

$$\frac{\partial \mathbf{w}_j^{A}\cdot\mathbf{w}_k^{B}}{\partial \alpha_i^{\Omega}} = D_{1k}^{B}\frac{\partial D_{1j}^{A}}{\partial \alpha_i^{\Omega}} + D_{1j}^{A}\frac{\partial D_{1k}^{B}}{\partial \alpha_i^{\Omega}} + D_{2k}^{B}\frac{\partial D_{2j}^{A}}{\partial \alpha_i^{\Omega}} + D_{2j}^{A}\frac{\partial D_{2k}^{B}}{\partial \alpha_i^{\Omega}} + D_{3k}^{B}\frac{\partial D_{3j}^{A}}{\partial \alpha_i^{\Omega}} + D_{3j}^{A}\frac{\partial D_{3k}^{B}}{\partial \alpha_i^{\Omega}} \tag{43}$$

In the rigid body case these terms are all zero due to the nondependence of the rotation matrices on the relative coordinates of the system atoms. In that alternate formalism the local frame is tied to the rigid molecule, and hence movement of the atoms of that system's molecules involve a concerted motion of all system atoms and the local coordinate frame does not change. However, in the flexible case, each atom of the system is able to move independently of the others and when such an atom is involved in the definition of an ALF, the derivative will be nonzero and contributions from the above equation must be taken into account.

These derivatives ($\partial q_k/\partial \alpha_i^{\Omega}$) are the same for all interaction tensor components for a given interaction, and so can be computed once and viewed as a set of coefficients for the other factor of eq 31, $\partial T_{\mathrm{AB}}/\partial q_k$, which is discussed next.

3.4.2. Derivatives of the Tensor Elements, $\partial T_{AB}/\partial q_k$. The first factor of eq 31 requires the derivatives of T_{AB} with respect to the scalar products. These are the same for the flexible as for the rigid case, but their description in the current context highlights some important points. According to ref.[46] the modified interaction tensor $\overline{T}$ is related to the interaction tensor T as follows, for $|k_a| \leq l_a$ and $|k_b| \leq l_b$,

$$T_{\pm k_{\mathrm{A}},\pm k_{\mathrm{B}}}^{l_{\mathrm{A}},l_{\mathrm{B}}} = N(l_{\mathrm{A}},k_{\mathrm{A}})N(l_{\mathrm{B}},k_{\mathrm{B}})R^{-L}\overline{T}_{k_{\mathrm{A}},k_{\mathrm{B}}}^{l_{\mathrm{A}},l_{\mathrm{B}}} \tag{44}$$

where $L = l_{\mathrm{A}} + l_{\mathrm{B}} + 1$ and N is a function only of the ranks of an AMM. By the product rule, the derivative of eq 44 with respect to any one of the 16 (= 1 + 3 + 3 + 9) possible scalar products q_j is

$$\frac{\partial T_{\pm k_{\mathrm{A}},\pm k_{\mathrm{B}}}^{l_{\mathrm{A}},l_{\mathrm{B}}}}{\partial q_j} = N(l_{\mathrm{A}},k_{\mathrm{A}})N(l_{\mathrm{B}},k_{\mathrm{B}})\left[R^{-L}\frac{\partial \overline{T}_{k_{\mathrm{A}},k_{\mathrm{B}}}^{l_{\mathrm{A}},l_{\mathrm{B}}}}{\partial q_j} + \overline{T}_{k_{\mathrm{A}},k_{\mathrm{B}}}^{l_{\mathrm{A}},l_{\mathrm{B}}}\frac{\partial R^{-L}}{\partial q_j}\right] \tag{45}$$

This can be simplified by making use of the relation

$$\frac{\partial R^{-L}}{\partial q_j} = \frac{\partial R^{-L}}{\partial R}\frac{\partial R}{\partial q_j} = -LR^{-L-1}\frac{\partial R}{\partial q_j} \tag{46}$$

which can be substituted into eq 31, resulting in the expression

$$\frac{\partial T_{\pm k_{\mathrm{A}},\pm k_{\mathrm{B}}}^{l_{\mathrm{A}},l_{\mathrm{B}}}}{\partial \alpha_i^{\Omega}} = N(l_{\mathrm{A}},k_{\mathrm{A}})N(l_{\mathrm{B}},k_{\mathrm{B}})R^{-L}\sum_{j=1}^{16}\frac{\partial q_j}{\partial \alpha_i^{\Omega}}\left[\frac{\partial \overline{T}_{k_{\mathrm{A}},k_{\mathrm{B}}}^{l_{\mathrm{A}},l_{\mathrm{B}}}}{\partial q_j} - \overline{T}_{k_{\mathrm{A}},k_{\mathrm{B}}}^{l_{\mathrm{A}},l_{\mathrm{B}}}LR^{-1}\frac{\partial R}{\partial q_j}\right] \tag{47}$$

It is possible to treat the problem as if the scalar products are independent of each other, i.e.

$$\frac{\partial q_i}{\partial q_j} = \delta_{ij} \quad \text{where} \quad \delta_{ij} = \begin{cases} 1 & \text{if} \quad i = j \\ 0 & \text{if} \quad i \neq j \end{cases} \tag{48}$$

All references consulted in the completion of this work employ the same independence of the scalar products when treating the rigid problem. The fact that this condition can be applied to the flexible case has been confirmed numerically in this work but not proven mathematically. A mathematical proof is desirable and should be carried out in future work. Utilizing eq 48, and rewriting the derivative of $R = (\mathbf{R}\cdot\mathbf{R})^{1/2}$ with respect to q_j in eq 47 leads to

$$\frac{\partial R}{\partial q_j} = \frac{\partial R}{\partial \mathbf{R}\cdot\mathbf{R}}\frac{\partial \mathbf{R}\cdot\mathbf{R}}{\partial q_j} = \frac{1}{2R}\frac{\partial \mathbf{R}\cdot\mathbf{R}}{\partial q_j} \tag{49}$$

This derivative (and thus the second term inside the square brackets of eq 47) is zero for all values of j in eq 48, except for j = 1 where it is equal to $1/2R$. The interaction tensor derivative can therefore be rewritten as

dx.doi.org/10.1021/ct500565g | J. Chem. Theory Comput. 2014, 10, 3840−3856

$$\frac{\partial T^{l_A,l_B}_{\pm k_A,\pm k_B}}{\partial \alpha_i^{\Omega}} = N(l_A,k_A)N(l_B,k_B)R^{-L}\left[\sum_{j=1}^{16}\left(\frac{\partial q_j}{\partial \alpha_i^{\Omega}}\frac{\partial \overline{T}^{l_A,l_B}_{k_A,k_B}}{\partial q_j}\right) - \frac{L}{2}R^{-2}\overline{T}^{l_A,l_B}_{k_A,k_B}\right] \tag{50}$$

The only remaining derivatives to compute are $\partial\overline{T}/\partial q_j (j = 1, ..., 16)$, which are conveniently computed using the recurrence relation given in work[46] (eq 24) by Hättig, depending on the value of the rank of the AMM on atom B. We distinguish two cases, namely, $l_B = 0$ and $l_B \neq 0$.

If $l_B = 0$ the recurrence relation is

$$\overline{T}^{l_A+1,0}_{k_A,0} = \frac{2l_A+1}{l_A+1}\sum_{\mu_A=1}^{3} M_{\mu_A,k_A} r^A_{\mu_A}\overline{T}^{l_A,0}_{\eta(\mu_A,k_A),0} - \frac{l_A}{l_A+1}\overline{T}^{l_A-1,0}_{k_A,0} \tag{51}$$

where M and η are given by tabulated values (Table 2 in ref 46) that are independent of the scalar products q_j (and hence act as constants when differentiating with respect to q_j). The derivative of eq 51 is taken via the product rule resulting in

$$\frac{\partial \overline{T}^{l_A+1,0}_{k_A,0}}{\partial q_j} = \frac{2l_A+1}{l_A+1}\sum_{\mu_A=1}^{3}\left[M_{\mu_A,k_A}\left(r^A_{\mu_A}\frac{\partial \overline{T}^{l_A,0}_{\eta(\mu_A,k_A),0}}{\partial q_j} + \overline{T}^{l_A,0}_{\eta(\mu_A,k_A),0}\frac{\partial r^A_{\mu_A}}{\partial q_j}\right)\right] - \frac{l_A}{l_A+1}\frac{\partial \overline{T}^{l_A-1,0}_{k_A,0}}{\partial q_j} \tag{52}$$

The derivatives of $\mathbf{r}^A$ require further description. Note that r^A_μ is the μ^{th} component of a unit vector, $\mathbf{r}^A$, which points from A to B and which is expressed in the ALF of atom A. To obtain this vector it is necessary to rotate the internuclear vector $\mathbf{R}$ from the global frame into the local frame and divide by its magnitude R. The global-to-local-rotation is achieved by multiplication of $\mathbf{R}$ by the rotation matrix $\mathbf{C}^A$. Then the j^{th} component of the $\mathbf{r}^A$ vector can be written

$$r^A_j = \frac{\mathbf{w}^A_j\cdot\mathbf{R}}{R} \tag{53}$$

Derivatives of this expression with respect to any of the 16 possible scalar products q_j can be found as follows. While details are provided in Appendix D (Supporting Information), a key result is

$$\frac{\partial r^A_j}{\partial q_j} = -\frac{r^A_j}{2R^2}\frac{\partial \mathbf{R}\cdot\mathbf{R}}{\partial q_j} + \frac{1}{R}\frac{\partial(\mathbf{w}^A_j\cdot\mathbf{R})}{\partial q_j} \tag{54}$$

from which the specific results, one for each type of q_j, can be readily obtained using the independence relation in eq 48.

The second case for the recurrence occurs when $l_B \neq 0$. In this case the interaction tensor is given by eq 25 in ref,[46]

$$\overline{T}^{l_A,l_B+1}_{k_A,k_B} = \overline{T}^{l_A-2,l_B+1}_{k_A,k_B} - \frac{2l_A+l_B}{l_B+1}\overline{T}^{l_A,l_B-1}_{k_A,k_B} + \frac{2l_A+2l_B+1}{l_B+1}\sum_{\mu_B=1}^{3} M_{\mu_B,k_B} r^B_{\mu_B}\overline{T}^{l_A,l_B}_{k_A,\eta(\mu_B,k_B)} + \frac{2l_A-1}{l_B+1}\sum_{\mu_A=1}^{3}\sum_{\mu_B=1}^{3} M_{\mu_A,k_A}M_{\mu_B,k_B}c^{AB}_{\mu_A,\mu_B}\overline{T}^{l_A-1,l_B}_{\eta(\mu_A,k_A),\eta(\mu_B,k_B)} \tag{55}$$

where $c^{AB}_{\mu_A,\mu_B}$ is a matrix describing an ALF to ALF rotation and will be defined later (see eq 57). Again the derivatives with respect to the scalar products can be taken by using the chain rule

$$\frac{\partial \overline{T}^{l_A,l_B+1}_{k_A,k_B}}{\partial q_j} = \frac{\partial \overline{T}^{l_A-2,l_B+1}_{k_A,k_B}}{\partial q_j} - \frac{2l_A+l_B}{l_B+1}\frac{\partial \overline{T}^{l_A,l_B-1}_{k_A,k_B}}{\partial q_j} + \frac{2l_A+2l_B+1}{l_B+1}\sum_{\mu_B=1}^{3}\left[M_{\mu_B,k_B}\left(r^B_{\mu_B}\frac{\partial \overline{T}^{l_A,l_B}_{k_A,\eta(\mu_B,k_B)}}{\partial q_j} + \overline{T}^{l_A,l_B}_{k_A,\eta(\mu_B,k_B)}\frac{\partial r^B_{\mu_B}}{\partial q_j}\right)\right] + \frac{2l_A-1}{l_B+1}\sum_{\mu_A=1}^{3}\sum_{\mu_B=1}^{3}\left[M_{\mu_A,k_A}M_{\mu_B,k_B}\left(c^{AB}_{\mu_A,\mu_B}\frac{\partial \overline{T}^{l_A-1,l_B}_{\eta(\mu_A,k_A),\eta(\mu_B,k_B)}}{\partial q_j} + \overline{T}^{l_A-1,l_B}_{\eta(\mu_A,k_A),\eta(\mu_B,k_B)}\frac{\partial c^{AB}_{\mu_A,\mu_B}}{\partial q_j}\right)\right] \tag{56}$$

Note that derivatives of $\mathbf{r}^B$ are discussed in Appendix D (Supporting Information).

The derivatives of $c^{AB}_{\mu_A,\mu_B}$ with respect to the scalar products are the final factor to be considered to make eq 56 derivative-free. These derivatives are zero unless the relevant scalar product (that the derivative is to be taken with respect to) is between two ALF unit vectors. In that case, the result can be either zero or one, depending on the scalar product pair involved. The matrix $\mathbf{c}_{AB}$ describes the rotation of a vector from the ALF of B to the ALF of A. It is therefore given by the product of the matrix that rotates a vector from the ALF of B to the global frame (denoted $\mathbf{D}_B$), and the matrix that rotates a vector from the global frame to the ALF of A (denoted $\mathbf{C}_A$),

$$\mathbf{c}^{AB} = \mathbf{C}^A\mathbf{D}^B = (\mathbf{D}^A)^T\mathbf{D}^B = (\mathbf{w}^A)^T\mathbf{w}^B \tag{57}$$

As previously described, the rotation matrices $\mathbf{D}^\Omega$ are composed of the unit vectors of the ALFs expressed in the global frame, $\mathbf{w}^\Omega_j$. Starting from eq 57, it can be shown that the i, j^{th} element of the matrix $\boldsymbol{c}^{AB}$is equal to the dot product $\mathbf{w}^A_i\cdot\mathbf{w}^B_j$. Thus, we can directly obtain the nonzero derivatives of the elements of $\boldsymbol{c}^{AB}$ from

$$\frac{\partial c^{AB}_{ij}}{\partial \mathbf{w}^A_k\cdot\mathbf{w}^B_l} = \begin{cases} 1 \text{ if } i = k \text{ and } j = l \\ 0 \text{ if } i \neq k \text{ or } j \neq l \end{cases} \tag{58}$$

where the independence relation of eq 48 can be used to show that derivatives with respect to the remaining seven scalar products are zero.

This is the final expression necessary for an implementation of the formulas needed to compute the atomic forces arising from the electrostatic interaction between atoms within a FF that has multipolar polarizable electrostatics. The next section describes the testing of the described formulas and the physical results found for a minimum energy conformation of alanine

dipeptide (AlaD) doubly capped with peptide bond, as shown in Figure 2.

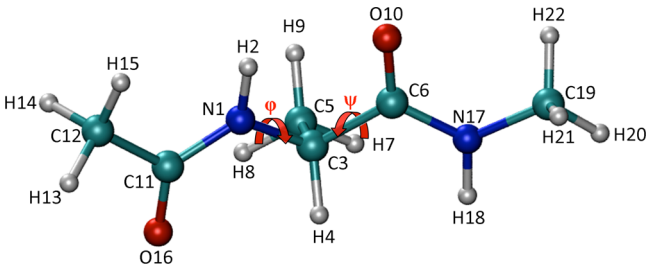

Figure 2. Structure of the AlaD molecule and the numbering system employed.

3.5. Testing of Electrostatic Forces Implementation.

The formulas for the forces described in the previous sections were implemented in Fortran 95. This choice was made on the basis that the majority of popular simulation packages are written in Fortran, removing the need for translation of the code prior to its incorporation in a molecular dynamics package. A nested approach was used, wherein each derived expression was implemented as a function, calling previously implemented functions when necessary (see the discussion of eqs B16 and B20 in Appendix B (Supporting Information) for an example). The implementation of the derivatives of the recurrence relations (eqs 51 and 55) is described in detail in the work of Rafat,[48] and the code from that implementation was employed herein. The combination of this with the flexible derivatives of the scalar products with respect to the global Cartesian coordinates of the nuclei allows computation of the tensor derivatives, and combining this with the derivatives of the moments it is possible to evaluate eq 8 analytically. The implementation was tested by comparison to finite difference results, wherein numerical differentiation was employed to confirm the correctness of the analytical derivatives. Finite difference derivatives were obtained for each function from the symmetrized formula

$$f'(x) \approx \frac{f(x+h) - f(x-h)}{2h} \tag{59}$$

where the error in the approximation depends on the value of h. There are two sources of error in computing this approximation to the derivative, namely, truncation error (due to terms left out of the Taylor expansion used to derive eq 59) and roundoff error (due to the accuracy of representation of numbers by the computer). These are discussed in further detail in Appendix E (Supporting Information), where justification of a value for h of 1×10^{-6} is given and deviations are discussed.

A single minimum energy conformation of the AlaD molecule (shown in Figure 3, provided in Appendix F, Supporting Information) was employed to test the implementation of the expressions for the electrostatic forces on the atoms. Calculating the electrostatic forces requires the global Cartesian coordinates, as well as specification of the ALF of each atom and a set of Kriging models to predict each AMM of each atom. The Kriging models and ALFs used herein are the same as those in previous work.[24,25] Full details of the construction and accuracy of the Kriging models can be found therein. For the purposes of testing of the analytical forces these details are actually not crucial because the calculation of

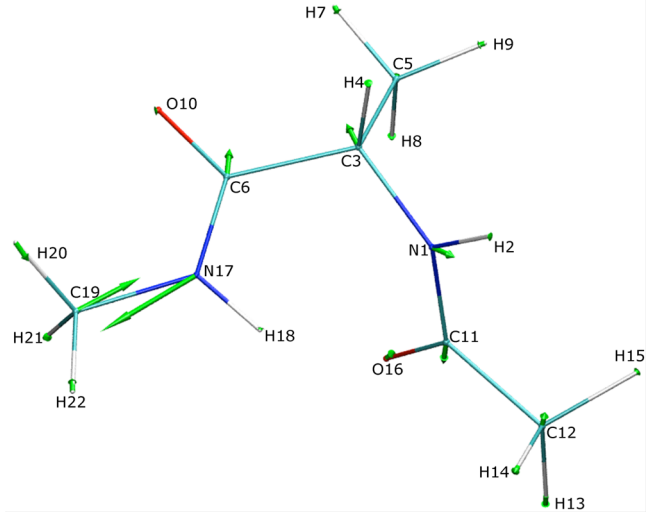

Figure 3. Conformation of AlaD used in the test on analytical forces. Atomic electrostatic force vectors are shown for each atom as arrows. The Cartesian coordinates for this conformation are given in Appendix F (Supporting Information).

the derivatives is general for any Kriging model. However, we reproduce some practical details here to increase familiarity with the QCTFF kriging methodology. At the HF/6-31G** level of theory there are 29 local energy minima for AlaD. Normal modes were computed for each of the minima. The data set was created by randomly distorting each minimum along a normal mode by a random factor, 100 times for each minimum. This produced 2900 distorted geometries, of which a thousand were sufficient to train and test the models, and 100 to test. Note that the test geometries are external to the set of training geometries. Reference 24 reports the performance of trained Kriging models by so-called S-curves, which show the logarithm of the absolute interaction energy error against their percentile values. Improvement of the models is manifested in leftward movement of the S-curve. The optimal number of training examples is unknown *a priori*, although 500 examples are sufficient for systems with numbers of atoms similar to AlaD. A sequence of Kriging models of increasing training set sizes, beginning at 100 and increasing in steps of 50, up to a maximum of 500 were built. This method allows the inspection of the developing accuracy of the models as more examples are added to the training set. It tuns out that a visually distinguishable improvement of the models up to a training set size of 250 examples. Thereafter, the progression is small and does not represent an improvement in every case. Finally, we note that training examples were filtered based on the magnitude of their integration errors,[49] measured by the values of $L(\Omega)$. Ideally, this quantity should be zero for all atoms; deviation from this value implies inaccurate integration of AMMs. The cutoff was set at 0.001 au.

Deviations of acceptable order of magnitude (for the applied value of h) were found for all implemented terms, thereby corroborating all analytical differentiations given above (and in Appendices A–D), as well as their implementation.

The results of the analytical evaluation of the electrostatic forces on the atoms of the test conformation are analyzed here to investigate the physical repercussions of the introduction of flexibility and polarization to the electrostatic term of the FF. Atomic electrostatic forces were computed for the described minimum energy conformation of AlaD (Figure 3) between all

dx.doi.org/10.1021/ct500565g | J. Chem. Theory Comput. 2014, 10, 3840–3856

Table 1. Atomic 1,4 and Higher Atomic Electrostatic Forces for the Atoms of a Single Conformation of AlaD

Ω	N1	H2	C3	H4	C5	C6	H7	H8	H9	O10	C11
$\lvert F^{\Omega}\rvert^a$	0.199	0.019	0.192	0.035	0.038	0.218	0.054	0.052	0.038	0.028	0.215
Ω	C12	H13	H14	H15	O16	N17	H18	C19	H20	H21	H22
$\lvert F^{\Omega}\rvert^a$	0.120	0.025	0.133	0.067	0.115	0.724	0.018	0.464	0.108	0.097	0.152

[a]Values are given in Hartree/Bohr.

atom pairs with a 1−4 (i.e., two atoms separated by three bonds) and higher relationship to each other. These are the electrostatic forces that would be computed during a calculation (e.g., a simulation or geometry optimization) that employs an FF that uses the described electrostatic potential in place of a charge−charge interaction. This approach also allows for the avoidance of convergence issues[50] that arise when using a multipolar expansion to evaluate short-range electrostatic interactions. Of the 231 possible atom−atom electrostatic interactions that occur in the 22 atom AlaD system, 174 interactions have a 1−4 or higher relationship between their atom pairs, and thus were included. The double sum over *A* and *B*, occurring in the force master equation eq 8, runs over all 174 interactions. The magnitudes of the individual atomic electrostatic force vectors for AlaD are given in Table 1.

A pictorial representation of the vectors F^{Ω} clarifies the physical meaning of the force values. These vectors are presented in Figure 3, where arrows indicate the global frame force vectors on each atom. The magnitudes of the vectors have been enhanced by a factor of 1.8 for visual clarity, but the relative magnitudes remain constant.

Figure 3 and Table 1 show that for this particular conformation the electrostatic force is greatest on atoms N17 and C19, with smaller (although same order of magnitude) relative forces on the remaining backbone atoms (N1, C3, C6, C11, C12, O16) and the hydrogen atoms of the methyl group containing C19. For the rest of the atoms (H2, H4, C5, H7, H8, H9, O10, H13, H14, H15, and H18) the atomic forces are significantly smaller (typically 1 order of magnitude).

As the considered conformation is a minimum, one may wonder why these forces do not vanish. In fact, electrostatic forces are but a part of the full atomic forces picture. The nonzero atom−atom electrostatic forces obtained through our method will be balanced by one of the other interactions at hand, as described by the full *ab initio* energy expression.

$$E_{\mathrm{tot}} = -\frac{1}{2}\sum_{\mathrm{A}}\int_{\Omega_{\mathrm{A}}} d\mathbf{r}_1 \nabla^2 \rho(\mathbf{r}_1, \mathbf{r}_2)|_{\mathbf{r}_1=\mathbf{r}_2} + \frac{1}{2}\sum_{\mathrm{A}}\sum_{\mathrm{B}}\int_{\Omega_{\mathrm{A}}} d\mathbf{r}_1 \int_{\Omega_{\mathrm{B}}} d\mathbf{r}_2 \frac{\rho_{\mathrm{tot}}(\mathbf{r}_1)\rho_{\mathrm{tot}}(\mathbf{r}_2)}{r_{12}} - \frac{1}{4}\sum_{\mathrm{A}}\sum_{\mathrm{B}}\int_{\Omega_{\mathrm{A}}} d\mathbf{r}_1 \int_{\Omega_{\mathrm{B}}} d\mathbf{r}_2 \frac{\rho(\mathbf{r}_1, \mathbf{r}_2)\rho(\mathbf{r}_2, \mathbf{r}_1)}{r_{12}} \quad (60)$$

This formula[51] refers to the total restricted Hartree−Fock electronic energy for a molecule, and is given in terms of the charge density $\rho_{\mathrm{tot}}(\mathbf{r})$ and the first-order reduced density matrix $\rho(\mathbf{r}_i,\mathbf{r}_j)$. The calculation of the potential energy terms was made possible for nonequilibrium geometries, for the first time thanks to previous work.[52] The nonelectrostatic terms in eq 60 (i.e., the exchange and kinetic energies) can also (in addition to the electrostatic terms) be predicted by carefully trained kriging models, as already demonstrated for atomic kinetic energies.[53] It should be noted that given a perfectly accurate model for prediction of the AMMs (and their derivatives) and a convergent expansion[44] of the electrostatic interaction energy (and its derivatives), the atomic forces computed via this method should match the QCT-partitioned *ab initio* forces. Deviation from the correct values can be traced back to the number of AMMs used to describe the electron distribution (i.e., the rank of the expansion); the interatomic distance (which must be sufficiently large to provide convergence at the chosen rank); and the deviation from perfect predictive behavior of the kriging models themselves.

Consideration of eq 8 shows that the atomic electrostatic force arising due to an interaction between a pair of atoms *A* and *B* consists of three types of contribution. The values of two of these contributions ($\partial Q^{\mathrm{A}}/\partial\alpha_i^{\Omega}$) are determined by the derivatives of the AMMs of the interacting atoms with respect to the global frame Cartesian coordinates of the atom Ω, α_i^{Ω} (see Section 3.1). The third contribution to eq 8 ($\partial T_{\mathrm{AB}}/\partial\alpha_i^{\Omega}$) is dependent on the derivatives of the interaction tensor components with respect to the same quantities α_i^{Ω} (see Section 3.4).

The former type of contribution can be connected to the polarization of the electrostatic representation employed. When an atom is displaced, the molecular electron distribution changes in response, resulting in a change in the AMMs *of all atoms*. The amount by which the AMMs of the interacting atoms *A* or *B* are altered by displacement of an atom Ω depends simultaneously on the nature of the atom on which they are centered (i.e., *A* or *B*), the nature of the atom that is displaced (i.e., Ω) and the chemical environment in which the change takes place (i.e., the nature of all other atoms present in the system). This deeply complex relationship between the system geometry and the AMMs is captured by the Kriging models that are assigned to the system. The AMM derivative terms $\partial Q^{\mathrm{A}}/\partial\alpha_i^{\Omega}$ do not occur in the rigid body, nonpolarizable case, hence the described effects are not captured.

The summation of the force contributions defined by eq 8 is complicated by the same intricate relationships between signed quantities as is found for the interaction energy. The complete sum for the derivative of the electrostatic interaction energy with respect to a particular atom Ω depends on the magnitude and sign of the AMMs of *A* and *B*, the derivatives of those AMMs with respect to global Cartesian coordinates,the interaction tensor and its derivatives with respect to global Cartesian coordinates. The physical picture that the electrostatic force describes is related to the polarizability of an atom, albeit through the Kriging model treatment rather than the usual response of an electron distribution to an external field. The derivatives of the AMMs of an atom *A* or *B* with respect to the coordinates of another atom Ω are a measure of how much the electron distribution of atom *A* or *B* is distorted by movement of atom Ω.

The magnitude of these derivatives provides a simultaneous indication of how polarizable the atom *A* or *B* is and how polarizing the atom Ω is. These two effects cannot be separated mathematically under the current treatment. The magnitude of the derivative is also expected to be dependent on the distance

Table 2. Magnitudes of Derivative Vectors of AMMs of Each Atom with Respect to the Global Frame Cartesian Coordinates of Atom N17 ($\partial Q_{lm}^{X}/\partial \alpha_i^{N17}$) for $l \leq 2$

X	Q_{00}	Q_{10}	Q_{11c}	Q_{11s}	Q_{20}	Q_{21c}	Q_{21s}	Q_{22c}	Q_{22s}
N1	0.000 76	0.003 40	0.001 20	0.004 70	0.082 00	0.003 80	0.110 00	0.009 00	0.000 16
H2	0.000 16	0.000 17	0.000 26	0.000 46	0.000 08	0.005 90	0.000 00	0.001 20	0.000 11
C3	0.021 00	0.003 00	0.000 60	0.120 00	0.062 00	0.017 00	0.011 00	0.110 00	0.035 00
H4	0.001 20	0.006 40	0.000 02	0.000 58	0.001 80	0.000 04	0.003 20	0.000 46	0.003 10
C5	0.005 20	0.000 81	0.003 10	0.001 70	0.006 80	0.002 40	0.002 40	0.005 40	0.001 30
C6	0.760 00	0.035 00	0.670 00	0.110 00	0.120 00	0.018 00	0.033 00	0.130 00	0.110 00
H7	0.000 43	0.000 08	0.000 03	0.003 60	0.033 00	0.001 50	0.001 20	0.001 90	0.003 20
H8	0.018 00	0.000 09	0.000 18	0.001 20	0.000 21	0.000 44	0.000 05	0.000 80	0.000 18
H9	0.000 49	0.000 02	0.000 01	0.001 00	0.000 54	0.003 00	0.008 10	0.000 27	0.001 50
O10	0.015 00	0.050 00	0.025 00	0.018 00	0.024 00	0.110 00	0.047 00	0.039 00	0.230 00
C11	0.000 31	0.000 06	0.000 23	0.001 10	0.000 28	0.000 08	0.000 26	0.000 43	0.000 34
C12	0.000 29	0.000 03	0.001 20	0.000 08	0.000 06	0.000 08	0.001 20	0.002 70	0.001 50
H13	0.000 21	0.000 27	0.000 07	0.000 01	0.000 13	0.000 00	0.000 15	0.000 17	0.000 00
H14	0.000 95	0.000 02	0.000 05	0.000 03	0.000 15	0.000 62	0.000 37	0.000 55	0.000 02
H15	0.000 54	0.000 03	0.000 04	0.000 04	0.000 09	0.000 03	0.000 05	0.000 09	0.000 17
O16	0.000 30	0.006 20	0.000 03	0.001 10	0.000 09	0.000 41	0.002 00	0.000 65	0.000 17
N17	0.840 00	0.048 00	0.830 00	0.330 00	1.400 00	1.500 00	2.200 00	0.740 00	0.270 00
H18	0.066 00	0.012 00	0.033 00	0.012 00	0.310 00	0.021 00	0.011 00	0.190 00	0.018 00
C19	2.000 00	0.058 00	1.000 00	0.015 00	0.130 00	0.120 00	0.092 00	0.130 00	0.310 00
H20	0.023 00	0.007 00	0.000 27	0.091 00	0.003 70	0.012 00	0.030 00	0.002 80	0.004 40
H21	0.010 00	0.004 90	0.000 54	0.065 00	0.011 00	0.008 80	0.002 60	0.073 00	0.017 00
H22	0.018 00	0.072 00	0.004 50	0.006 40	0.004 20	0.009 40	0.003 30	0.029 00	0.028 00

between the pair of atoms, where the effect of displacement of Ω on the AMMs of *A* or *B* is expected to be inversely proportional to the interatomic separation. In the case of the test case AlaD molecule, there are 22 atoms, each of which has its electron distribution described by 9 AMMs (up to the atomic quadrupole moment $l = 2$). Each of the 9 AMMs of each atom has a derivative with respect to displacement of all 22 system atoms along three Cartesian axes, giving a total of 13 068 ($= 3 \times [(3 \times 22)^2]$) derivatives that contribute to the final atomic electrostatic forces. To investigate the physical origins and implications of the results it is therefore necessary to select a subset of this information. We choose to analyze the atom N17 as it experiences the largest 1−4 and higher electrostatic force of all the atoms of this conformation (see Table 1 and Figure 3).

First, the polarizing effect of N17 on the other atoms of the system is considered. This is assessed by observation of the amount of change caused to an AMM of atom Ω by displacement of the atom N17. The three space coordinates mean that this is a vector of three elements, each one denoted $\partial Q_{lm}^{\Omega}/\partial \alpha_i^{N17}$ ($i = 1, 2, 3$; Ω = 1, 2, ..., 22) and so we report the magnitude of this vector only. The results are collected in Table 2 for $l \leq 2$.

The results of this calculation are physically straightforward. The tabulated values depend on two derivatives (see eq 9): those of the molecule's features with respect to the coordinates of N17 ($\partial f_k/\partial \alpha_i^{N17}$), and those of the AMMs of the atoms with respect to the molecule's features ($\partial Q^{\Omega}/\partial f_k$). The first of these is a geometric effect and thus depends on the ALF relationship between the differentiated atom Ω and N17, and is independent of the particular AMM (i.e., it does not depend on *l* or *m*, and as such needs to only be evaluated once to obtain all AMM derivatives for a given atom). It is sensible, based on the discussion of the possible relationships given in Appendix B (Supporting Information), to infer that the contribution of this term to derivatives of AMMs of an atom Ω for which N17 is an ALF-defining atom will be larger than those where there is no relationship.

The second term in eq 9, the dependence of the AMMs on the feature values ($\partial Q^{\Omega}/\partial f_k$) is a more chemical relationship. We can infer that this relationship depends on both the polarizing nature of N17, and the polarizability of the atom Ω whose AMMs are to be differentiated, where both factors are dependent on the chemical system in which they exist. By considering derivatives with respect to N17 (as we do in Table 2) we may assume that the observations we make are made against a constant polarizing effect from the N atom; that is, for any interaction *A*−*B* that we look at, the type of atom Ω (which the differentiation is done with respect to) will be N for each observation. Thus, the observations we make may change for another set of interactions where Ω is a different type, but for the results here we can compare by element of atom *A* or *B* and obtain insight into the polarizability of these atoms under a roughly constant polarizing influence from N17. Therefore, the AMM derivatives of atoms with larger contributions from this factor will be those that are "softer" (i.e., more polarizable), as well as closer to N17 in space.

Consideration of Table 2 shows that the most significant derivatives of Q_{00}^{Ω} with respect to $\boldsymbol{\alpha}^{N17}$ are found for the atoms N17, C6, and C19, all at least 1 order of magnitude greater than the next nearest derivative. There are also appreciable values for C3, H8, O10, H18 and the methyl group H20, H21 and H22, all of which are several orders of magnitude greater than the values found for the remaining atoms (N1, H2, H4, C5, H7, H9, C11, C12, H13, H14, H15, and O16). The fact that N17, C6, and C19 have the largest derivatives is explained by the fact that all three are involved in the definition of the ALF of N17. This relationship means that a large geometrical contribution to the derivative is made. In addition, the fact that these 3 atoms are members of the ALF of N17 implies a small distance between the atoms, which increases the effect on the derivatives

dx.doi.org/10.1021/ct500565g | J. Chem. Theory Comput. 2014, 10, 3840−3856

Table 3. Magnitudes of Derivative Vectors of the AMMs of Atom N17 with Respect to Global Frame Cartesian Coordinates of Each Atom of the Test AlaD Conformation ($\partial Q_{lm}^{X}/\partial \alpha_i^{N17}$)

X	Q_{00}	Q_{10}	Q_{11c}	Q_{11s}	Q_{20}	Q_{21c}	Q_{21s}	Q_{22c}	Q_{22s}
N1	0.000 43	0.004 90	0.000 36	0.001 60	0.000 26	0.002 00	0.004 20	0.003 20	0.004 70
H2	0.001 20	0.000 06	0.001 20	0.003 10	0.003 10	0.002 40	0.001 30	0.003 70	0.002 60
C3	0.000 20	0.007 20	0.005 20	0.003 10	0.009 80	0.041 00	0.250 00	0.120 00	0.170 00
H4	0.000 17	0.019 00	0.000 81	0.008 10	0.000 94	0.002 50	0.000 52	0.001 10	0.001 30
C5	0.005 10	0.000 56	0.001 50	0.000 36	0.003 10	0.000 13	0.002 30	0.002 70	0.004 30
C6	0.880 00	0.011 00	0.750 00	0.052 00	0.940 00	0.540 00	0.350 00	0.560 00	0.068 00
H7	0.000 08	0.003 00	0.001 70	0.001 20	0.001 70	0.001 30	0.000 96	0.001 70	0.000 67
H8	0.000 00	0.001 40	0.001 60	0.000 07	0.000 93	0.000 59	0.001 40	0.000 69	0.005 20
H9	0.001 90	0.000 03	0.000 16	0.000 03	0.002 10	0.000 49	0.002 80	0.000 23	0.002 40
O10	0.031 00	0.003 90	0.019 00	0.030 00	0.037 00	0.012 00	0.018 00	0.038 00	0.100 00
C11	0.000 74	0.000 53	0.000 78	0.000 37	0.001 10	0.000 41	0.000 96	0.004 00	0.012 00
C12	0.001 00	0.000 58	0.000 18	0.003 50	0.000 48	0.002 10	0.000 75	0.000 23	0.001 60
H13	0.000 44	0.000 20	0.000 91	0.000 35	0.000 43	0.000 18	0.000 69	0.000 77	0.001 10
H14	0.000 77	0.001 30	0.000 56	0.004 10	0.000 34	0.000 13	0.000 52	0.000 31	0.001 60
H15	0.000 22	0.000 20	0.000 30	0.000 01	0.000 16	0.000 44	0.000 89	0.000 11	0.001 40
O16	0.000 02	0.002 10	0.001 30	0.000 20	0.005 70	0.000 48	0.001 90	0.004 60	0.002 00
N17	0.840 00	0.048 00	0.830 00	0.330 00	1.400 00	1.500 00	2.200 00	0.740 00	0.270 00
H18	0.022 00	0.017 00	0.031 00	0.046 00	0.520 00	0.770 00	0.780 00	0.140 00	0.050 00
C19	0.540 00	0.030 00	0.220 00	0.480 00	0.590 00	0.400 00	0.840 00	0.200 00	0.085 00
H20	0.004 00	0.011 00	0.027 00	0.002 00	0.007 90	0.007 30	0.035 00	0.092 00	0.000 15
H21	0.060 00	0.023 00	0.002 60	0.087 00	0.001 70	0.018 00	0.015 00	0.068 00	0.002 90
H22	0.002 10	0.001 20	0.007 50	0.034 00	0.004 20	0.003 60	0.004 70	0.051 00	0.006 60

of the AMM models. For the atoms O10, H18, H20, H21, and H22 the same argument can be made, as N17 is used to define a member of the ALF of each of these atoms. The ALFs of H8 and C3 do not use N17 in their definition, and as such the magnitude of the AMM derivatives cannot be explained by geometrical contributions. C3 is in close proximity to N17 in both a bond-graph and a "through space" manner, and so is expected to be polarized by N17. The larger derivative for H8 (and the fact it is clearly different from its methyl-forming partners H7 and H9) suggests that there is a structural effect at play. Consultation of Figure 3 suggests that H7 and H9 may be screened by the presence of H4, whereas H8 experiences no such effect. The remainder of the atoms are distant from N17 and that atom is not involved in defining their ALFs, explaining the small derivatives of their AMMs with respect to displacing N17

An alternative (opposite) perspective is given by consideration of how much the atom N17 is polarized (i.e., how much its AMMs are altered) by displacement of the atoms of the system, i.e. the values of $\partial Q_{lm}^{N17}/\partial \alpha_i^{\Omega}$. These values give an idea of how, for a given polarizability, the polarization effect of the atom Ω determines the magnitude of the AMM derivative vectors. The values for the test conformation are collected in Table 3. The same physical phenomenon is reported as in Table 2, that is, the magnitude of the derivative vector of each AMM. However, the derivative is now taken with respect to the Cartesian coordinates of each of the molecule's atoms, rather than just N17, i.e. the reported values are the magnitudes of the vectors $\partial Q_{lm}^{N17}/\partial \alpha_i^{\Omega}$ (i = 1, 2, 3; Ω = 1, 2, ..., 22). Of course, the N17 row in Table 3 is exactly the same as the N17 row in Table 2 (both correspond to the magnitude of the vector $\partial Q_{lm}^{N17}/\partial \alpha_i^{\Omega}$).

In contrast to Table 2, when considering the values in Table 3 we note that it is now important to ask whether N17 is a member of the ALFs of each of the system atoms, Ω. The geometric factor in the AMM derivatives is now $\partial f_k/\partial \alpha_i^{\Omega}$, where f_k are the features that describe the system from the point of view of N17. If the atom Ω is not a member of the ALF of N17, then these derivatives will be zero, except for the derivatives of the features that describe atom Ω specifically. Only displacement of the three ALF atoms N17, C6, and C19 affects the features expressed in the ALF of N17 related to atoms other than Ω, as they result in a change in the ALF itself. Examination of Table 3 shows that the values of $\partial Q_{lm}^{N17}/\partial \alpha_i^{\Omega}$ for these three atoms are significantly in excess of those of other atoms. The polarization contribution is also significant because C6 and C19 have a 1−2 relationship with N17. For the rest of the derivatives it is only necessary to consider the element of the atom and how distant it is from N17 as the only nonzero feature derivatives will be those of the three spherical polar coordinates that specify the position of Ω in the ALF of N17. Invoking the concept of chemical hardness[54] assists in the discussion. Nitrogen is viewed as a hard atom, and thus the derivatives with respect to the non-ALF atoms are expected to be small. Atom H18 (covalently bonded to N17) is expected to have the largest derivative outside of the ALF atoms, and this is indeed a large value relative to all other hydrogen atoms, excepting H21 and H9. The other atoms in close proximity to N17 (H20, H21, H22, O10) give relatively larger derivatives of its AMMs ($\partial Q_{lm}^{N17}/\partial \alpha_i^{\Omega}$) compared to the more distant remainder of the molecule.

In summary, the analysis of Tables 2 and 3 clearly show the two effects at hand: that the AMM derivatives can be rationalized as being composed of a geometric part, dependent on the ALF relationship between A, B, and Ω; and a polarization part, depending on both the chemical nature of the atoms involved and on their environment.

The interaction tensor derivatives, $\partial T_{AB}/\partial \alpha_i^{\Omega}$, (the central factor of the middle term in eq 8) describe the geometric dependence of the interaction between the set of AMMs of the

interacting atoms *A* and *B*. This derivative accounts for how the orientation of the atomic local frames of two interacting atoms contributes to the atomic forces. This assertion suggests that when the nuclear position of a particular atom Ω influences the interaction energy it does so via being involved in the definition of the local frame of one or both of the interacting atoms. There is no contribution to the force from this effect when Ω is not an ALF atom as all derivatives are then zero (see eq 31).

The mathematical nature of the tensor derivative term depends on the relationship between the atoms *A*, *B*, and Ω. More specifically, this term depends on whether Ω is used in the definition of the ALF of either interacting atom, *A* or *B*. As considered in Section 3, for any interaction, Ω may be equal to one of *Ao*, *Ax*, *Axy* or none of the atoms defining the ALF of *A*, denoted *G*. It can also be equal to one of *Bo*, *Bx*, and *Bxy* or none of the ALF-defining atoms of *B*. The only pair that Ω cannot simultaneously be equal to is *A* (*Ao*) and *B* (*Bo*), due to the fact that an atom is not considered to have an electrostatic interaction with itself in this part of the FF. This is because the intra-atomic Coulomb energy is not treated with multipole moments in QCTFF. In the rigid body case, all derivatives of the tensor are zero except for those taken with respect to the interacting atoms *A* and *B*. This is a special case of the problem for the flexible case, which is illuminated by construction of all possible combinations, shown in Table 4. In this table, Ω is equal to the column and row headings simultaneously. Each table entry refers to the derivative of the tensor for the interaction between *A* and *B* with respect to the atom Ω. Each entry portrays Ω in two ways: by the ALF centered on *A* and by the ALF centered on *B*. For each ALF there are four possibilities that can be independently varied: *Ao*, *Ax*, *Axy*, or *G*.

Table 4. Nature of Tensor Derivatives for Different Relationships between *A*, *B*, and Ω

Ω[a]	*Ao*	*Ax*	*Axy*	*G*
Bo		R/F	R/F	R/F
Bx	R/F	F	F	F
Bxy	R/F	F	F	F
G	R/F	F	F	zero

[a]The role of Ω in defining the ALF of atom *A* is given by the heading of the column, and its role in defining the ALF of *B* is given by the heading of the row. The letter "R" indicates that the derivative is non-zero in the rigid body formalism, while "F" indicates that the derivative is non-zero in the flexible case.

The pattern of Rs (rigid body) in Table 4 shows that, for the rigid case, the tensor derivatives only do not vanish if Ω is at the origin of the ALF of either *A* (column of Rs) or *B* (row of Rs). For a flexible molecule, the derivatives of the interaction tensor will be different to those of a rigid body as an additional eight terms (corresponding to the eight cells of Table 4 that contain only the entry F) must be considered. This is captured by the mathematics as described in Section 3.4, where we note that there can be physical effects arising from the dependence on all the ALF atoms' positions (geometrical changes possible in flexible case). The size of the contribution from the central term of eq 8 depends on the relationship between *A*, *B*, and Ω, since the derivative $\partial q_j/\partial \alpha_i^{\Omega}$ is a factor in each term of the tensor derivative (see eq 47), and these factors are zero if the atom Ω is not a member of the ALF of *A* or *B*.

As a final analysis of the electrostatic atomic forces for the test conformation, we note that the terms arising in the sum over interacting pairs *A* and *B* can be separated into two types as follows. The total force on an atom Ω is made up of contributions from the derivatives of each interaction in the system (see the sum over *AB* in eq 8). The interactions can be grouped into those which the atom Ω is directly involved in (i.e., Ω = *A* or *B*) and those in which it is not involved (i.e., Ω ≠ *A* and Ω ≠ *B*). The former type is the familiar atom−atom force, where an atom *A* is considered to exert a force on atom *B* by virtue of their energetic interaction. The latter type involves the exertion of a force on Ω as a result of the interaction between two other atoms. These contributions arise when there is some dependence of the interaction between *A* and *B* on the position of a third atom. This effect can be a result of both the polarizable definition of the electrostatic interaction and the dependence of the ALFs of system atoms on the positions of atoms other than themselves. To compare these two types of interaction and evaluate how much separation exists between them in physical terms, the contributions to the force on atom N17 from each interaction *AB* can be compared. Atom N17 is directly involved in 13 1−4 and higher electrostatic interactions in AlaD (see Figure 3), and therefore there are 174 − 13 = 161 interactions in which N17 is not directly involved. Figure 4 plots the distributions of the two types of contribution to the force on atom N17. Note the logarithmic scale on the *y*-axis.

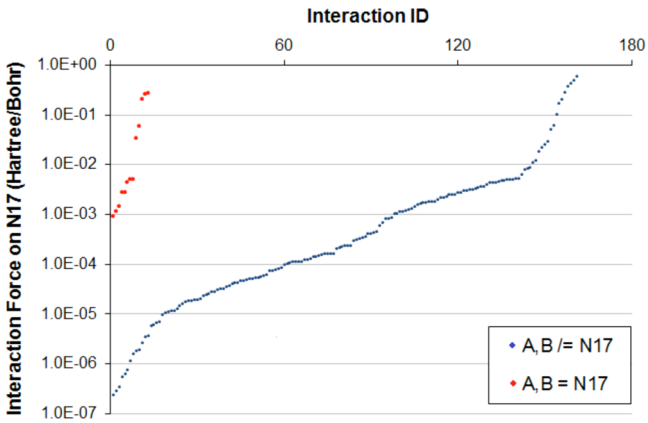

Figure 4. Force contributions from individual atom−atom interactions to the total electrostatic force on atom N17, grouped according to whether the interaction involves N17 (*A*, *B* = N17, red) or not (*A*, *B* ≠ N17, blue). Note the 13 red dots, corresponding to the 13 1−4 and higher interacting pairs in which N17 appears. Note that the *x*-axis is a "dummy" axis in that it is an arbitrary counter.

Clearly, from this plot, the interactions involving N17 all make a significant relative contribution to the total force on the atom. However, such interactions do not dominate the sum and a number of other interactions make relatively similar and greater contributions to the total. The latter interactions are those where N17 causes a significant polarization of one or both of the interacting atoms, or where N17 is involved in defining the ALF of one or both of the interacting atoms. Further delineation of the interactions according to their ALF properties is possible. The larger tail of the plotted blue points (i.e., the region where the force is of similar magnitude to interactions involving N17) is composed exclusively of interactions involving the atoms C6, C19, and H18, which are directly bonded to N17 in the AlaD molecule, and two of

which define the ALF of N17. There are four points (none of which correspond to an interaction that includes N17) that each make a larger contribution to the total force on N17 than the single largest contribution from an interaction that *does* involve N17. These four points all correspond to interactions between atom C19 and other protein backbone atoms (specifically O16, N1, C11, and (largest of all) O10). Thus, the force contributions on atom N17 from interactions in which it is not directly involved are significant, and when not included (i.e., when polarization and flexibility effects are ignored) then a different physical picture will be recovered.

In future work, the electrostatic forces will be combined with nonelectrostatic forces, again obtained within the QCTFF framework, inspired by eq 60. Since the first calculation of the Coulomb energy between topological atoms,[52] a coherent piece of work on topological energy partitioning emerged,[55−57] in parallel with other such work[51,58,59] presenting a minimal and rigorous picture of atomic energetic behavior in any system. This approach offers an appealing route to replace the energy terms of classical FFs, such as intermolecular repulsion (Buckingham-type potentials), from the elementary mono- and diatomic energy contributions that topological energy partitioining defines. Within this framework, all-energy forces can be obtained, after which geometry optimization can be carried out. In a more ambitious stage, a molecular dynamics simulation can be conducted, which is a subject of current research in our lab.

4. CONCLUSION

We derived fully analytical expressions of the atomic electrostatic forces for high-rank multipolar electrostatics with full polarization by the machine learning method kriging. All expressions were corroborated by the finite difference method. The force is expressed as a sum over pairs of interacting atoms. The individual contributions to the total atomic forces are significantly different from those of the rigid-body nonpolarizable paradigm, involving contributions from both polarization of the system charge density and the flexibility of the molecule. Forces on individual atoms are composed of contributions from all interactions in the system. Three terms appear in the expression for each contribution. Two of these involve the derivatives of atomic multipole moments and involve products of geometrical and polarization factors. The third involves the derivative of the interaction tensor and is purely geometric. The magnitude of the contribution from a specific interaction depends on an intricate combination of the chemical nature of the interacting and displaced atoms, the environment in which they exist, and the relationship between atoms defining their local frames. The test-case study of the doubly peptide-capped amino acid alanine is discussed at length.

■ ASSOCIATED CONTENT

Supporting Information

Six appendices: (a) handling the normalized data (input and output) that Kriging models are based on, (b) differentiation of all features with respect to Cartesian displacement coordinates, (c) differentiation of Cartesian coordinates in an ALF with respect to Cartesian displacement coordinates (in the global frame) (d) differentiation of the internuclear unit vector r^A in the ALF frame with respect to Cartesian displacement coordinates (in the global frame) or $\partial r_j^A/\partial q_j$, (e) finite differences, and (f) test conformation. This material is available free of charge via the Internet at http://pubs.acs.org/.

■ AUTHOR INFORMATION

Corresponding Author

*E-mail: paul.popelier@manchester.ac.uk. Phone: +44 161 3064511.

Present Address

[§]Dept. of Chemistry, Univ. of Southern California, 3620 McClintock Avenue, Los Angeles, CA 90089, United States

Notes

The authors declare no competing financial interest.

■ ACKNOWLEDGMENTS

M.J.L.M. thanks the EPSRC for a DTA Ph.D. studentship. The authors thank Dr. F. Zielinski for useful feedback and T. J. Hughes for assistance with graphics.

■ REFERENCES

(1) Cisneros, G. A.; Karttunen, M.; Ren, P.; Sagui, C. Classical Electrostatics for Biomolecular Simulations. *Chem. Rev.* **2014**, *114*, 779−814.

(2) Raval, A.; Piana, S.; Eastwood, M. P.; Dror, R. O.; Shaw, D. E. Refinement of protein structure homology models via long, all-atom molecular dynamics simulations. *Proteins: Struct., Funct., Bioinf.* **2012**, *80*, 2071−2079.

(3) Cardamone, S.; Hughes, T. J.; Popelier, P. L. A. Multipolar Electrostatics. *Phys. Chem. Chem. Phys.* **2014**, *16*, 10367−10387.

(4) Panhuis, M. I. H.; Popelier, P. L. A.; Munn, R. W.; Angyan, J. G. Distributed polarizability of the water dimer: Field-induced charge transfer along the hydrogen bond. *J. Chem. Phys.* **2001**, *114*, 7951−7961.

(5) Holt, A.; Boström, J.; Karlström, G.; Lindh, R. A NEMO potential that includes the dipole−quadrupole and quadrupole−quadrupole polarizability. *J. Comput. Chem.* **2010**, *31*, 1583−1591.

(6) Chaudret, R.; Gresh, N.; Parisel, O.; Piquemal, J. P. Many-Body Exchange-Repulsion in Polarizable Molecular Mechanics. I. Orbital-Based Approximations and Applications to Hydrated Metal Cation Complexes. *J. Comput. Chem.* **2011**, *32*, 2949−2957.

(7) Ren, P. Y.; Wu, C. J.; Ponder, J. W. Polarizable Atomic Multipole-Based Molecular Mechanics for Organic Molecules. *J. Chem. Theory Comput.* **2011**, *7*, 3143−3161.

(8) Vinter, J. G. Extended Electron Distributions Applied to the Molecular Mechanics of some Intermolecular Interactions. *J. Comput.-Aided Mol. Des.* **1994**, *8*, 653−668.

(9) Ghosh, D.; Kosenkov, D.; Vanovschi, V.; Williams, C. F.; Herbert, J. M.; Gordon, M. S.; Schmidt, M. S.; Slipchenko, L. V. Noncovalent Interactions in Extended Systems Described by the Effective Fragment Potential Method: Theory and Application to Nucleobase Oligomers. *J. Phys. Chem. A* **2010**, *114*, 12739−12754.

(10) Price, S. L.; Leslie, M.; Welch, G. W. A.; Habgood, M.; Price, L. S.; Karamertzanis, P. G.; Day, G. M. Modelling organic crystal structures using distributed multipole and polarizability-based model intermolecular potentials. *Phys. Chem. Chem. Phys.* **2010**, *12*, 8478−8490.

(11) Hodges, M. P.; Stone, A. J.; Xantheas, S. S. Contribution of Many-Body Terms to the Energy for Small Water Clusters: A Comparison of ab Initio Calculations and Accurate Model Potentials. *J. Phys. Chem. A* **1997**, *101*, 9163−9168.

(12) Kumar, R.; Wang, F.-F.; Jenness, G.; Jordan, K. A. A second generation distributed point polarizable water model. *J. Chem. Phys.* **2010**, *132*, 014309.

(13) Wheatley, R. J.; Mitchell, J. B. O. Gaussian Multipoles in Practice: Electrostatic Energies for Intermolecular Potentials. *J. Comput. Chem.* **1994**, *15*, 1187−1198.

(14) Volkov, A.; King, H. F.; Coppens, P.; Farrugia, L. On the calculation of the electrostatic potential, electric field and electric field gradient from the aspherical pseudoatom model. *Acta Crystallogr., Sect. A: Found. Crystallogr.* **2006**, *62*, 400−408.
(15) Popelier, P. L. A. A generic force field based on Quantum Chemical Topology. In *Modern Charge-Density Analysis;* Gatti, C., Macchi, P., Eds.; Springer: Germany, 2012; Vol. *14*; pp 505−526.
(16) Popelier, P. L. A. Quantum Chemical Topology: Knowledgeable Atoms in Peptides. *AIP Conf. Proc.* **2012**, *1456*, 261−268.
(17) Bader, R. F. W. *Atoms in Molecules. A Quantum Theory;* Oxford Univ. Press: Oxford, Great Britain, 1990.
(18) Popelier, P. L. A. Quantum Chemical Topology: on Bonds and Potentials. In *Structure and Bonding. Intermolecular Forces and Clusters;* Wales, D. J., Ed.; Springer: Heidelberg, Germany, 2005; Vol. *115*, pp 1−56.
(19) Koch, U.; Popelier, P. L. A.; Stone, A. J. Conformational Dependence of Atomic Multipole Moments. *Chem. Phys. Lett.* **1995**, *238*, 253−260.
(20) Krige, D. G. A statistical approach to some basic mine valuation problems on the Witwatersrand. *J. Chem., Metall. Min. Soc. S. Afr.* **1951**, *52*, 119−139.
(21) Rasmussen, C. E.; Williams, C. K. I. *Gaussian Processes for Machine Learning;* The MIT Press: Cambridge, MA, 2006.
(22) Handley, C. M.; Hawe, G. I.; Kell, D. B.; Popelier, P. L. A. Optimal Construction of a Fast and Accurate Polarisable Water Potential based on Multipole Moments trained by Machine Learning. *Phys. Chem. Chem. Phys.* **2009**, *11*, 6365−6376.
(23) Mills, M. J. L.; Popelier, P. L. A. Intramolecular polarisable multipolar electrostatics from the machine learning method Kriging. *Comput. Theor. Chem.* **2011**, *975*, 42−51.
(24) Mills, M. J. L.; Popelier, P. L. A. Polarisable multipolar electrostatics from the machine learning method Kriging: an application to alanine. *Theor. Chem. Acc.* **2012**, *131*, 1137−1153.
(25) Kandathil, S. M.; Fletcher, T. L.; Yuan, Y.; Knowles, J.; Popelier, P. L. A. Accuracy and Tractability of a Kriging Model of Intramolecular Polarizable Multipolar Electrostatics and Its Application to Histidine. *J. Comput. Chem.* **2013**, *34*, 1850−1861.
(26) Mills, M. J. L.; Hawe, G. I.; Handley, C. M.; Popelier, P. L. A. Unified approach to multipolar polarisation and charge transfer for ions: microhydrated Na+. *Phys. Chem. Chem. Phys.* **2013**, *15*, 18249−18261.
(27) Rupp, M.; Tkatchenko, A.; Mueller, K.-R.; von Lilienfeld, O. A. Fast and Accurate Modeling of Molecular Atomization Energies with Machine Learning. *Phys. Rev. Lett.* **2012**, *108*, 058301.
(28) Bartok, A.; Payne, M. C.; Kondor, R.; Csanyi, G. Gaussian Approximation Potentials: The Accuracy of Quantum Mechanics, without the Electrons. *Phys. Rev. Lett.* **2010**, *104*, 136403.
(29) Snyder, J. C.; Rupp, M.; Hansen, K.; Mueller, K. R.; Burke, K. Finding Density Functionals with Machine Learning. *Phys. Rev. Lett.* **2012**, *108*, 253002−1−5.
(30) Handley, C. M.; Popelier, P. L. A. Potential Energy Surfaces Fitted by Artificial Neural Networks. *J. Phys. Chem. A* **2010**, *114*, 3371−3383.
(31) Behler, J.; Parrinello, M. Generalized Neural-Network Representation of High-Dimensional Potential-Energy Surfaces. *Phys. Rev. Lett.* **2007**, *98*, 146401.
(32) Behler, J. Representing potential energy surfaces by high-dimensional neural network potentials. *J. Phys.: Condens. Matter* **2014**, *26*, 183001.
(33) Liem, S. Y.; Popelier, P. L. A. Properties and 3D structure of liquid water: a perspective from a high-rank multipolar electrostatic potential. *J. Chem. Theory Comput.* **2008**, *4*, 353−365.
(34) Liem, S. Y.; Popelier, P. L. A.; Leslie, M. Simulation of liquid water using a high rank quantum topological electrostatic potential. *Int. J. Quantum Chem.* **2004**, *99*, 685−694.
(35) Shaik, M. S.; Liem, S. Y.; Popelier, P. L. A. Properties of Liquid Water from a Systematic Refinement of a High-rank Multipolar Electrostatic Potential. *J. Chem. Phys.* **2010**, *132*, 174504.
(36) Shaik, M. S.; Liem, S. Y.; Yuan, Y.; Popelier, P. L. A. Simulation of Liquid Imidazole Using a High-Rank Quantum Topological Electrostatic Potential. *Phys. Chem. Chem. Phys.* **2010**, *12*, 15040−15055.
(37) Liem, S.; Popelier, P. L. A. High Rank Quantum Topological Electrostatic Potential: Molecular Dynamics Simulation of Liquid HF. *J. Chem. Phys.* **2003**, *119*, 4560−4566.
(38) Liem, S. Y.; Shaik, M. S.; Popelier, P. L. A. Aqueous imidazole solutions: a structural perspective from simulations with high-rank electrostatic multipole moments. *J. Phys. Chem. B* **2011**, *115*, 11389−11398.
(39) Liem, S. Y.; Popelier, P. L. A. The hydration of serine: multipole moments versus point charges. *Phys. Chem. Chem. Phys.* **2014**, *16*, 4122−4134.
(40) Popelier, P. L. A.; Stone, A. J. Formulae for the first and second derivatives of anisotropic potentials with respect to geometrical parameters. *Mol. Phys.* **1994**, *82*, 411−425.
(41) Simmonett, A. C.; Pickard, F. C.; S, H. F., III; Brooks, B. R. An efficient algorithm for multipole energies and derivatives based on spherical harmonics and extensions to particle mesh Ewald. *J. Chem. Phys.* **2014**, *140*, 184101.
(42) Zielinski, F.; Popelier, P. L. A. Spherical tensor multipolar electrostatics and smooth particle mesh Ewald summation: a theoretical study. *J. Mol. Graphics Modell.* **2014**, *20*, 2256−2273.
(43) Stone, A. J. *The Theory of Intermolecular Forces,* 1st ed.; Clarendon Press: Oxford, U.K., 1996; Vol. *32*.
(44) Popelier, P. L. A.; Joubert, L.; Kosov, D. S. Convergence of the Electrostatic Interaction Based on Topological Atoms. *J. Phys. Chem. A* **2001**, *105*, 8254−8261.
(45) Price, S. L.; Stone, A. J.; Alderton, M. Explicit formulae for the electrostatic energy, forces and torques between a pair of molecules of arbitrary symmetry. *Mol. Phys.* **1984**, *52*, 987−1001.
(46) Haettig, C. Recurrence relations for the direct calculation of spherical multipole interaction tensors and Coulomb-type interaction energies. *Chem. Phys. Lett.* **1996**, *260*, 341−351.
(47) Popelier, P. L. A.; Stone, A. J.; Wales, D. J. Topography of Potential-energy Surfaces for van der Waals Complexes. *Faraday Discuss.* **1994**, *97*, 243−264.
(48) Rafat, M. How to cut molecular energy with golden scissors. M.Sc. Dissertation, U.M.I.S.T, 2002.
(49) Aicken, F. M.; Popelier, P. L. A. Atomic properties of selected biomolecules. Part 1. The interpretation of atomic integration errors. *Can. J. Chem.* **2000**, *78*, 415−426.
(50) Rafat, M.; Popelier, P. L. A. A convergent multipole expansion for 1,3 and 1,4 Coulomb interactions. *J. Chem. Phys.* **2006**, *124*, 144102−1−7.
(51) Rafat, M.; Popelier, P. L. A. Atom-atom partitioning of total (super)molecular energy: the hidden terms of classical force fields. *J. Comput. Chem.* **2007**, *28*, 292−301.
(52) Popelier, P. L. A.; Kosov, D. S. Atom-atom partitioning of intramolecular and intermolecular Coulomb energy. *J. Chem. Phys.* **2001**, *114*, 6539−6547.
(53) Fletcher, T. L.; Kandathil, S. M.; Popelier, P. L. A. The prediction of atomic kinetic energies from coordinates of surrounding atoms using kriging machine learning. *Theor. Chem. Acc.* **2014**, *133*, 1499:1−10.
(54) Parr, R. G.; Pearson, R. G. Absolute Hardness—Companion Parameter to Absolute Electronegativity. *J. Am. Chem. Soc.* **1983**, *105*, 7512−7516.
(55) Blanco, M. A.; Pendas, A. M.; Francisco, E. Interacting Quantum Atoms: A Correlated Energy Decomposition Scheme Based on the Quantum Theory of Atoms in Molecules. *J. Chem. Theory Comput.* **2005**, *1*, 1096−1109.
(56) Pendas, A. M.; Francisco, E.; Blanco, M. A. Binding Energies of First Row Diatomics in the Light of the Interacting Quantum Atoms Approach. *J. Phys. Chem. A* **2006**, *110*, 12864−12869.
(57) Pendás, A. M.; Blanco, M. A.; Francisco, E. The nature of the hydrogen bond: A synthesis from the interacting quantum atoms picture. *J. Chem. Phys.* **2006**, *125*, 184112−1−20.

(58) Darley, M. G.; Popelier, P. L. A. Role of Short-Range Electrostatics in Torsional Potentials. *J. Phys. Chem. A* **2008**, *112*, 12954−12965.
(59) Rafat, M.; Popelier, P. L. A.: Topological atom-atom partitioning of molecular exchange energy and its multipolar convergence. In *Quantum Theory of Atoms in Molecules;* Matta, C. F., Boyd, R. J., Eds.; Wiley-VCH: Weinheim, Germany, 2007; Vol. *5*, pp 121−140.